Title: Neuroendocrine control of the proteostatic network by HPK-1 delays aging

Authors: Maria I. Lazaro-Pena[1], Carlos A. Diaz-Balzac[2], Ritika Das[1,3,4], Andrew Samuelson[1*]

Affiliations:
[1] Department of Biomedical Genetics, University of Rochester Medical Center, Rochester, New York, USA

[2] Division of Endocrinology, Diabetes and Metabolism, Department of Medicine, University of Rochester Medical Center, Rochester, New York, USA

[3] Department of Biology, University of Rochester, Rochester, New York, USA

[4] Department of Cell Biology, Skirball Institute of Biomolecular Medicine, NYU School of Medicine, New York, New York, USA.

* Corresponding author. Andrew_Samuelson@URMC.Rochester.edu

Abstract:

The nervous system systemically coordinates proteostasis to maintain organismal health. In this work, we identify the transcriptional cofactor HPK-1 (homeodomain-interacting protein kinase) as a key neuronal component of the proteostatic network: its overexpression produces a paracrine signal to hyper-induce molecular chaperones and a neuroendocrine signal to induce autophagy in peripheral tissues. Neuronal HPK-1 signaling improves proteostasis in distal tissues through neurotransmitters. These pro-longevity modalities are independently regulated within serotonergic and GABAergic neurons, respectively, through distinct adaptive responses, either of which improve proteostasis in a cell non-autonomous manner. The former protects the proteome from acute stress while the latter fortifies the proteome to delay aging. Thus, HPK-1 acts as a central regulatory node upstream of the greater PN, exerting complementary roles in distinct neuronal cell-types.

One-Sentence Summary: Neuronal control of proteostasis and aging

Main Text:

Cellular aging throughout an organism is characterized by the gradual decline of the proteome (proteostasis), which precipitates the onset and progression of a growing number of age-associated diseases (*1-3*). Proteostatic decline corresponds with the age-associated breakdown of a large proteostasis network (PN), which coordinates stress-responsive control of protein folding, degradation, and translation in response to myriad cell intrinsic and non-autonomous signals. An increasing number of studies have implicated the nervous system as a key regulator of organismal proteostasis (*4*), yet how this is achieved remains obscure.

The transcriptional cofactor HPK-1 (homeodomain-interacting protein kinase 1) extends organismal longevity and prevents the decline in proteostasis. This involves at least two distinct mechanisms: stimulating chaperone gene expression via the heat shock transcription factor 1 (HSF-1) and bolstering autophagy in response to decreased activity of the Target of Rapamycin Complex 1 (TORC1) (*5*). In this study, we sought to dissect how HPK-1 modulates organismal proteostasis and aging at the tissue and cellular level.

We sought to determine the tissues where HPK-1 exerts a regulatory control of longevity. Transgenic animals overexpressing *hpk-1* in either muscular, intestinal, or hypodermal cells had a normal longevity (fig. S1A-C). In contrast, neuronal overexpression of *hpk-1* was sufficient to significantly increase lifespan by 17%, a modest amount comparable to constitutive overexpression of *hpk-1* throughout the soma (Fig. 1A) (*5*). Because *hpk-1* null mutant animals are short-lived, and aging correlates with

decreased movement (*5-7*), we performed a locomotion assay. *hpk-1(pk1393)* null mutants displayed a reduced number of body bends at day 2 of adulthood (Fig. 1B). Overexpression of *hpk-1* in neurons was sufficient to mitigate the locomotion defect of *hpk-1* null mutants. We and others previously found that in the absence of *hpk-1*, animals are vulnerable to acute thermal stress (*5, 7*). Restoring *hpk-1* expression solely within the nervous system was sufficient to fully rescue the reduced thermotolerance of *hpk-1* null mutant animals (Fig. 1C). We conclude that *hpk-1* primarily acts within the nervous system to promote longevity, health span, and thermal stress resistance.

To determine whether *hpk-1* is important to preserve the anatomy and physiology of the nervous system during aging, we examined the role of *hpk-1* in the maintenance of neuronal structure. To assess age-associated changes in neuroanatomy of ventral and dorsal cord motor neurons (VD and DD), we used the *unc-25p::GFP* cell-specific reporter (Fig. 1D) (*8*). By more than a 3-fold difference, aged populations of *hpk-1* mutant animals displayed more VD and DD axonal breaks compared to wild type animals (Fig. 1E, fig. S2A), and age-associated breaks could be rescued by neuronal expression of *hpk-1* (Fig. 1F). Importantly, young wild-type and *hpk-1* mutant animals did not show neuronal breaks. Thus, loss of *hpk-1* does not disrupt axon formation during development, rather HPK-1 preserves axonal integrity in aging motor neurons. To examine the role of *hpk-1* in synaptic transmission, we performed a paralysis assay after acetylcholinesterase inhibition with aldicarb, where mutations that impair cholinergic signaling cause a reduction in rate of paralysis. *hpk-1* mutants showed increased aldicarb resistance (Fig. 1G), suggesting that loss of *hpk-1* reduces cholinergic synaptic transmission. *C. elegans* serotonin (5-HT) signaling regulates a number of behaviors, including locomotion, and

animals treated with exogenous 5-HT exhibit paralysis over time. In a paralysis assay with exogenous 5-HT, we observed that *hpk-1* mutants paralyzed faster, suggesting a role for *hpk-1* in the regulation of serotonin signaling (fig. S2B). Thus, *hpk-1* is essential for the proper maintenance of neuronal processes and synaptic transmission.

Based on these observations, we postulated two possibilities that are not mutually exclusive. First, HPK-1 functions in neurons to cell intrinsically improve neuronal integrity and its proteome, consequently promoting longevity and health of the animal. Second, neuronal HPK-1 activates a cell extrinsic signal to regulate proteostasis in distal tissues. To test the first possibility, we investigated the regulation of proteostasis by measuring polyglutamine aggregate formation in neuronal cells (*rgef-1p::Q40::YFP*) of animals overexpressing *hpk-1* pan-neuronally (*rab-3p::hpk-1*). Animals overexpressing *hpk-1* within neurons showed a slight decreased number of fluorescent foci within the nerve ring (Fig. 2A*i* - *iii*,B). To assess whether this was associated with improved neuronal function, we assessed alterations in locomotion capacity (body bends) after placement in liquid. Neuronal *hpk-1* overexpression significantly increased the average number of body bends of the *rgef-1p::Q40::YFP* animals (17.7 $\pm$ 1 vs 12.5 $\pm$ 1.2 bends/30sec), suggesting that neuronal expression of *hpk-1* improves proteostasis in the nervous system and mitigates locomotion defects associated to the decline in proteostasis (Fig. 2C). We next tested whether HPK-1 was necessary to preserve proteostasis within neurons. We crossed the *rgef-1::Q40::YFP* reporter with the neuronal enhanced RNAi *sid-1(pk3321);unc-119p::sid-1* strain and assessed whether neuronal inactivation of *hpk-1* hastened age-associated proteostatic decline. Animals with neuronal *hpk-1* inactivation had a significant increase in foci number within neurons and a decreased number of body

bends in liquid (19.7 ± 0.8 vs 25.5 ± 1.1 bends/30sec) (Fig. 2A*iv*,D,E). Thus, HPK-1 functions cell intrinsically to maintain neuronal proteostasis.

We next asked whether neuronal HPK-1 regulates proteostasis in muscles, which are synaptically connected to neurons. Muscle is a main receiver of neuronal signaling, in the locomotion of multicellular organisms. To investigate whether HPK-1 activity in neurons regulates distal muscle proteostasis, we used a proteostasis reporter expressed exclusively in muscle tissue (*unc-54p::Q35::YFP*). Animals with increased neuronal *hpk-1* expression had significantly decreased fluorescent foci in muscle tissue. For instance, at day 3 of adulthood, animals overexpressing neuronal HPK-1 had an average of 21 ± 0.9 polyQ aggregates, while control animals had an average of 26 ± 1.1 polyQ aggregates (Fig. 2F*i,ii*,G). In *C. elegans*, the age-related progressive proteotoxic stress of muscle polyQ expression is pathological and results in paralysis. Of note, *hpk-1* overexpression in neurons was sufficient to reduce paralysis; at day 13 of adulthood only 61% ± 0.10 of neuronal *hpk-1* overexpressing animals were paralyzed compared to 81% ± 0.08 of paralyzed control animals (Fig. 2H). Conversely, neuronal inactivation of *hpk-1* (*sid-1(pk3321); unc-119p::sid-1; unc-54p::Q35::YFP; hpk-1(RNAi)*) was sufficient to hasten the collapse of proteostasis, significantly increasing the number of polyQ aggregates (45 ± 1 vs 32 ± 1.1 at day 4) and paralysis rate (84% ± 0.04 vs 14% ± 0.04 at day 9) (Fig. 2F*iii*,I,J). Thus, HPK-1 functions within the nervous system regulates proteostasis in distal muscle tissue, which implies that HPK-1 coordinates organismal health through cell non-autonomous mechanisms.

To identify the signaling mechanism employed by HPK-1 to regulate distal proteostasis, we tested whether mutant animals impaired for neuropeptide and

neurotransmitter transmission are essential for cell non-autonomous regulation of proteostasis (*unc-31* and *unc-13* mutants, respectively Fig. 2K). Neuronal expression of *hpk-1* in *unc-31* mutants improved proteostasis in the absence of neuropeptide transmission (Fig. 2L). In contrast, in the absence of neurotransmitter function, neuronal expression of *hpk-1* in *unc-13* mutants failed to improve proteostasis in muscle tissue (Fig. 2M). Thus, neuronal cell non-autonomous signaling occurs through neurotransmitter transmission.

We sought to identify the components of the PN that are cell non-autonomously regulated via HPK-1 activity in the nervous system. *hpk-1* is required for the induction of molecular chaperones after heat shock and the induction of autophagy after nutrient stress (*5*). We tested whether neuronal HPK-1 overexpression alters the expression of molecular chaperones (*hsp-16.2p::GFP*). Neuronal overexpression of HPK-1 in wild type animals did not alter the basal expression of molecular chaperones (fig. S3A). In contrast, after heat shock, neuronal *hpk-1* overexpression increased *hsp-16.2p::GFP* expression, particularly in the pharynx and head muscles but not intestinal cells (Fig. 3A,B, fig. S3B,C). We conclude that while *hpk-1* is required for the broad induction of molecular chaperones, neuronal HPK-1 primes inducibility of the heat shock response (HSR) within specific tissues, rather than in a systemic manner throughout the organism. We next tested whether increased neuronal HPK-1 activity is sufficient to induce autophagy. Using two LGG-1/Atg8 fluorescent reporter strains to visualize autophagosome levels in neurons (*rgef-1p::LGG-1::GFP)* and hypodermal seam cells (*lgg-1p::LGG-1::GFP)*, we found that neuronal *hpk-1* over expression significantly induces autophagy in both the nervous system (fig. S4A) and in hypodermal seam cell (Fig. 3C,D), but not in the intestine

(fig. S4B). Thus, increased HPK-1 activity within the nervous system acts to induce autophagy both cell-intrinsically and non-autonomously.

To begin to identify the specific neuronal cell-types from which neuronal HPK-1 initiates distinct cell non-autonomous signals, we overexpressed HPK-1 in different subtypes of neurons and assessed changes in muscle proteostasis (*unc-54p::Q35::YFP*). *hpk-1* overexpression in glutamatergic and dopaminergic neurons was not sufficient to decrease the formation of fluorescent foci or reduce paralysis (fig. S5). In contrast, overexpression of *hpk-1* in either serotonergic (*tph-1p::hpk-1*) or GABAergic (*unc-47p::hpk-1*) neurons was sufficient to improve proteostasis in muscle tissue and reduce paralysis (Fig. 4A-D). Accordingly, we found that *hpk-1* is expressed in serotonergic and GABAergic neurons, based on colocalization between *hpk-1* and serotonergic and GABAergic cell-type specific reporters (Fig. 4E-H, fig. S6), which suggests that HPK-1 initiates pro-longevity signals from these neurons to preserve muscle proteostasis.

We sought to determine whether signals initiated from serotonergic and GABAergic neurons induced similar or distinct components of the PN in distal tissues, and the overall consequence on organismal health. Since pan-neuronal expression of HPK-1 was sufficient to induce autophagy, improve thermotolerance, and increase lifespan, we chose to focus on these three phenotypes. Increased HPK-1 serotonergic signaling was sufficient to improve thermotolerance, without altering autophagy or lifespan (Fig. 4I-K). In contrast, increased HPK-1 expression in GABAergic neurons did not alter thermotolerance, but induced autophagy and slightly increased lifespan (Fig. 4L-N, fig. S7). Thus, HPK-1 initiated distinct signals from serotonergic and GABAergic neurons to improve organismal health. Specifically, HPK-1 initiates serotonergic signals

to improve survival to acute thermal stress and GABAergic signals that increases basal autophagy to increase lifespan in the absence of stress (Fig. 4O).

A growing number of studies have demonstrated the nervous system plays a pivotable role in the regulation of overall organismal health and longevity in response to metabolic, environmental, and intrinsic cues (*4*). We find that increased HPK-1 activity in serotonergic neurons does not increase lifespan, but improves muscle proteostasis and amplify the expression of molecular chaperones. Previous findings have discovered that serotoninergic neurons receive stress signals from the thermosensory circuit, which regulate HSF-1 activity in the germline (*9*). Serotonin signaling is essential for the induction of the HSR (*9, 10*). Our results are analogous with a previous finding that demonstrated HSF-1 regulation of the HSR through thermosensory circuits is separable from lifespan (*11*). HPK-1 co-localizes with HSF-1 in neurons and is also essential for induction of the HSR (*5, 11*). Collectively, we posit HPK-1-dependent signaling from serotonergic neurons functions as a component of the thermosensory circuit, which acts in conjunction with HSF-1 to restore proteostasis in response to acute damage within the proteome.

Increased HPK-1 activity in GABAergic neurons induces autophagy in peripheral cells, improves proteostasis and longevity. We posit this occurs via antagonism of GABA signaling. Loss of GABA increases *C. elegans* lifespan (*12, 13*). GABA signaling in mice inhibits autophagy and causes oxidative stress, which is mitigated via Tor1 inhibition (*14*). Neuronal expression of HPK-1 is inhibited by TORC1 and *hpk-1* is essential for loss of TORC1 to extend longevity and induce autophagy gene expression (*5*). TORC1 acts within neurons to regulate aging (*15*). Collectively, our results position HPK-1 activity in

GABAergic neurons as the likely integration point for cell non-autonomous metabolic regulation of autophagy via TORC1 activity.

This work reveals a new level of specificity in the capacity of the nervous system to initiate adaptive responses by triggering distinct components of the proteostatic network across cell types. Elucidating how neuronal cell-types generate heterotypic signals to coordinate the maintenance of homeostasis are just beginning to emerge. Our work demonstrates differential, yet specific, activation of cytosolic components of the PN in separate peripheral tissues, further underscoring how the nervous system of metazoans integrate diverse stimuli to activate specific adaptive responses to maintain homeostasis.

References:

1. A. J. Sala, L. C. Bott, R. I. Morimoto, Shaping proteostasis at the cellular, tissue, and organismal level. *J Cell Biol* **216**, 1231-1241 (2017).
2. R. I. Morimoto, The heat shock response: systems biology of proteotoxic stress in aging and disease. *Cold Spring Harb Symp Quant Biol* **76**, 91-99 (2011).
3. R. I. Morimoto, Cell-Nonautonomous Regulation of Proteostasis in Aging and Disease. *Cold Spring Harbor perspectives in biology*, (2019).
4. H. A. Miller, E. S. Dean, S. D. Pletcher, S. F. Leiser, Cell non-autonomous regulation of health and longevity. *Elife* **9**, (2020).
5. R. Das *et al.*, The homeodomain-interacting protein kinase HPK-1 preserves protein homeostasis and longevity through master regulatory control of the HSF-1 chaperone network and TORC1-restricted autophagy in Caenorhabditis elegans. *PLoS Genet* **13**, e1007038 (2017).
6. A. V. Samuelson, C. E. Carr, G. Ruvkun, Gene activities that mediate increased life span of C. elegans insulin-like signaling mutants. *Genes Dev* **21**, 2976-2994 (2007).
7. S. Berber *et al.*, Homeodomain-Interacting Protein Kinase (HPK-1) regulates stress responses and ageing in C. elegans. *Scientific reports* **6**, 19582 (2016).
8. H. Cinar, S. Keles, Y. Jin, Expression profiling of GABAergic motor neurons in Caenorhabditis elegans. *Curr Biol* **15**, 340-346 (2005).
9. M. C. Tatum *et al.*, Neuronal serotonin release triggers the heat shock response in C. elegans in the absence of temperature increase. *Curr Biol* **25**, 163-174 (2015).

10. V. Prahlad, T. Cornelius, R. I. Morimoto, Regulation of the cellular heat shock response in Caenorhabditis elegans by thermosensory neurons. *Science* **320**, 811-814 (2008).
11. P. M. Douglas *et al.*, Heterotypic Signals from Neural HSF-1 Separate Thermotolerance from Longevity. *Cell Rep* **12**, 1196-1204 (2015).
12. L. Chun *et al.*, Metabotropic GABA signalling modulates longevity in C. elegans. *Nature communications* **6**, 8828 (2015).
13. F. Yuan *et al.*, GABA receptors differentially regulate life span and health span in C. elegans through distinct downstream mechanisms. *Am J Physiol Cell Physiol* **317**, C953-C963 (2019).
14. R. Lakhani *et al.*, Defects in GABA metabolism affect selective autophagy pathways and are alleviated by mTOR inhibition. *EMBO Mol Med* **6**, 551-566 (2014).
15. Y. Zhang *et al.*, Neuronal TORC1 modulates longevity via AMPK and cell nonautonomous regulation of mitochondrial dynamics in C. elegans. *Elife* **8**, (2019).

Acknowledgements:

We would like to thank members of the Samuelson laboratory, past and present, for their thoughtful insight in many discussions related to this project. In this regard, we would particularly like to thank Adam Cornwell. We would like to thank members of the Western New York Worm Group for their input. We would like to thank Dr. Doug Portman (URMC) and his laboratory for strains and advice. Some strains were provided by the CGC, which is funded by NIH Office of Research Infrastructure Programs (P40 OD010440). We would like to personally thank Drs. Dirk Bohmann (URMC) and Gary Ruvkun (MGH/HMS) for critical reading of this manuscript. Research reported in this publication was supported by the National Institute On Aging of the National Institutes of Health under Award Number RF1AG062593. CADB was supported by F32HD105323. The content is solely the responsibility of the authors and does not necessarily represent the official views of the National Institutes of Health.

Fig 1

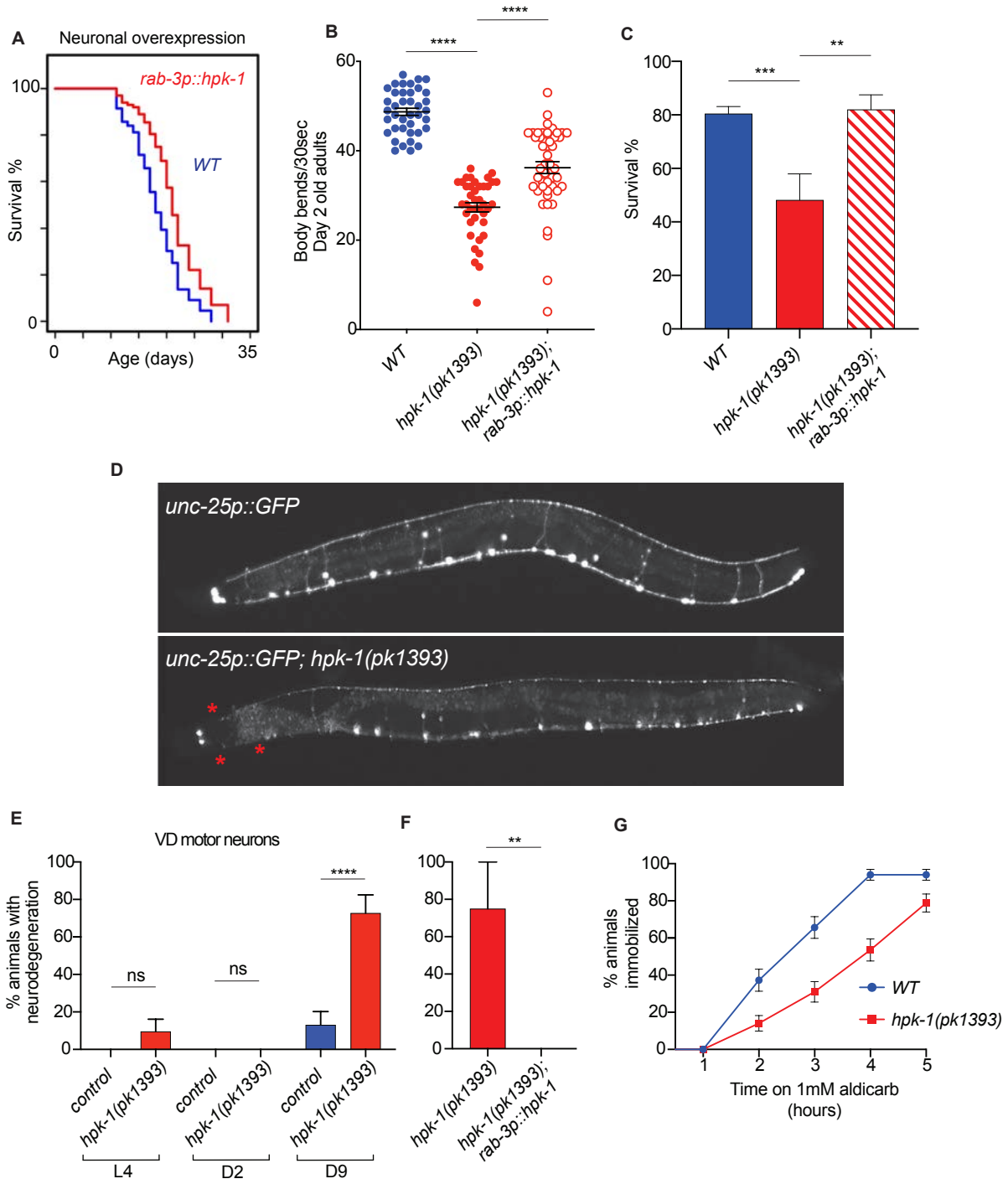
A
Neuronal overexpression
rab-3p::hpk-1
WT
Survival %
100
0
0
Age (days)
35
B
****
****
Body bends/30sec
Day 2 old adults
60
40
20
0
WT
hpk-1(pk1393)
hpk-1(pk1393);
rab-3p::hpk-1
C
***
**
Survival %
100
80
60
40
20
0
WT
hpk-1(pk1393)
hpk-1(pk1393);
rab-3p::hpk-1
D
unc-25p::GFP
unc-25p::GFP; hpk-1(pk1393)
E
VD motor neurons
% animals with
neurodegeneration
ns
ns
****
control
hpk-1(pk1393)
control
hpk-1(pk1393)
control
hpk-1(pk1393)
L4
D2
D9
F
**
hpk-1(pk1393)
hpk-1(pk1393);
rab-3p::hpk-1
G
% animals
immobilized
WT
hpk-1(pk1393)
Time on 1mM aldicarb
(hours)
1
2
3
4
5

Fig 1. Neuronal HPK-1 extends longevity and maintains neuronal integrity.

(A) Survival curves of animals overexpressing *hpk-1* in the nervous system compared with control non-transgenic siblings. Lifespan is representative of two independent biological replicates ($n \geq 175$, $P < 0.0001$). **(B)** Frequency of body bends of *wild type*, *rab-3p::hpk-1* and *hpk-1(pk1393); rab-3p::hpk-1* animals maintained ($n \geq 48$). **(C)** Survival of animals subjected to heat shock treatment. Graph represents one of the two individual trials ($n \geq 66$). **(D)** Fluorescent micrographs of control and *hpk-1(pk1393)* old adults animals expressing GFP in GABAergic DD and VD motor neurons. Asterisks (*) indicate axonal breaks in the motor neurons. **(E)** Percentage of animals with neurodegeneration in VD motor neurons ($n \geq 23$). **(F)** Percentage of animals with neurodegeneration in VD motor neurons ($n \geq 10$). **(G)** Percentage of immobilized animals after exposure to aldicarb ($n \geq 67$). *T* test analysis with $^{**}P < 0.01$ and $^{***}P < 0.001$. See Supplemental Tables: 1, 3, 5, 8, and 9 for details and additional trials.

Fig 2

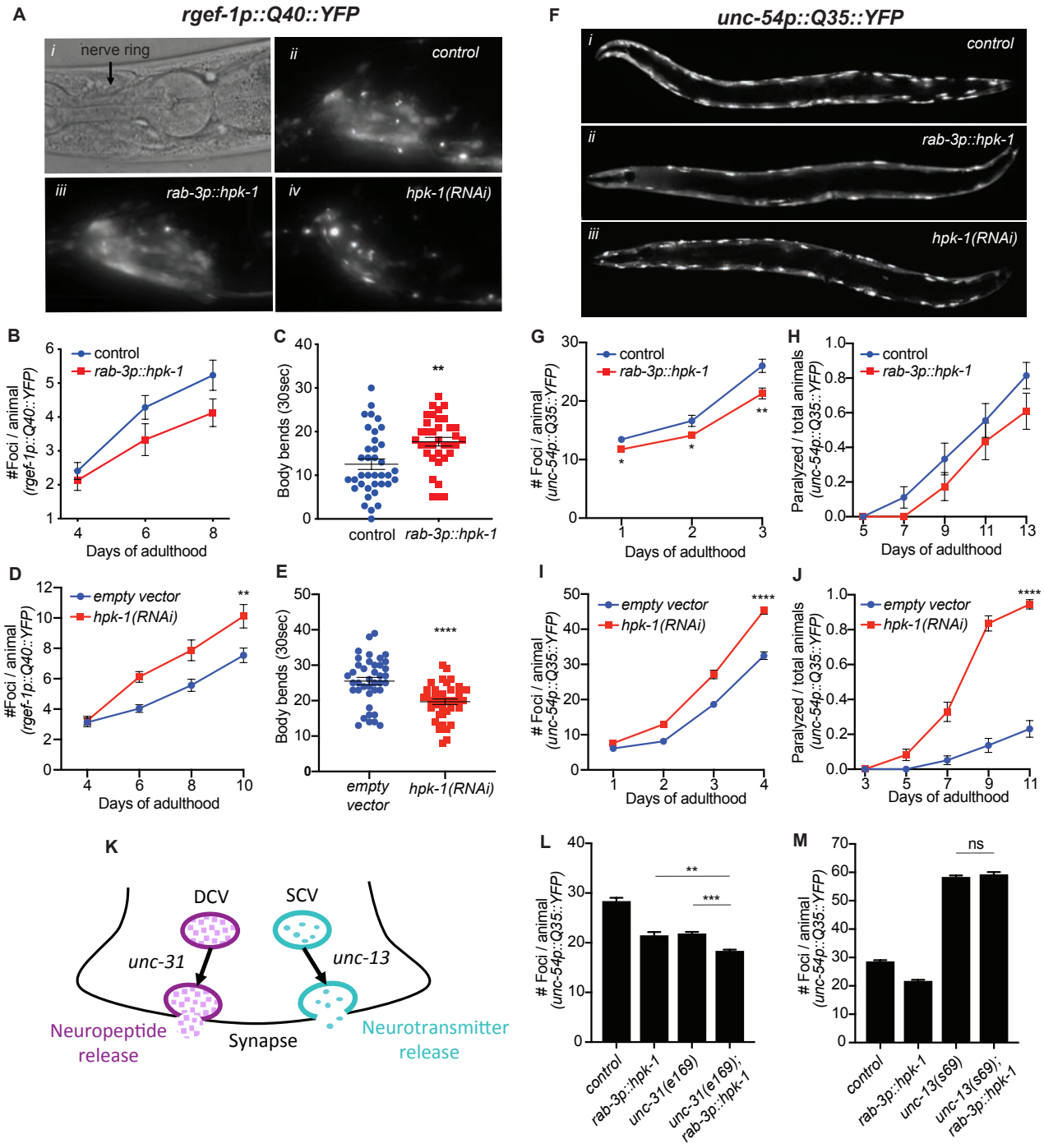
A
rgef-1p::Q40::YFP
i
nerve ring
ii
control
iii
rab-3p::hpk-1
iv
hpk-1(RNAi)
F
unc-54p::Q35::YFP
i
control
ii
rab-3p::hpk-1
iii
hpk-1(RNAi)
B
control
rab-3p::hpk-1
#Foci / animal (rgef-1p::Q40::YFP)
Days of adulthood
C
Body bends (30sec)
control
rab-3p::hpk-1
G
Foci / animal (unc-54p::Q35::YFP)
Days of adulthood
H
Paralyzed / total animals (unc-54p::Q35::YFP)
Days of adulthood
D
empty vector
hpk-1(RNAi)
#Foci / animal (rgef-1p::Q40::YFP)
Days of adulthood
E
Body bends (30sec)
empty vector
hpk-1(RNAi)
I
Foci / animal (unc-54p::Q35::YFP)
Days of adulthood
J
Paralyzed / total animals (unc-54p::Q35::YFP)
Days of adulthood
K
DCV
SCV
unc-31
unc-13
Neuropeptide release
Synapse
Neurotransmitter release
L
Foci / animal (unc-54p::Q35::YFP)
control
rab-3p::hpk-1
unc-31(e169)
unc-31(e169); rab-3p::hpk-1
M
ns
Foci / animal (unc-54p::Q35::YFP)
control
rab-3p::hpk-1
unc-13(s69)
unc-13(s69); rab-3p::hpk-1

Fig 2. Neuronal HPK-1 prevents the decline in proteostasis through neurotransmitter release.

(A) Nomarski (*i*) and fluorescent (*ii-i v*) micrographs of animals expressing polyglutamine fluorescent reporter within the nervous system. (**B** and **C**) Quantification of foci in the nerve ring (B) and body bend frequency (C) ($n \geq 21$ for B and $n \geq 36$ for C). (**D** and **E**) Quantification of foci in the nerve ring (D) and frequency of body bends (E) in neuronal enhanced RNAi animals ($n \geq 19$ for D and $n \geq 39$ for E). **(F)** Fluorescent micrographs of animals expressing the polyglutamine fluorescent reporter in muscle. (**G** and **H**) Quantification of foci in muscle (G) and paralysis rate (H). Graphs are representative of 5 individual transgenic lines ($n \geq 18$ for G and $n \geq 23$ for H). (**I** and **J**) Quantification of foci in muscle (I) and paralysis rate (J) in neuronal enhanced RNAi animals ($n \geq 22$ for I and $n \geq 73$ for J). **(K)** Neuropeptides and neurotransmitters are essential for neuronal signaling; vesicle release depends on *unc-31* and *unc-13*, respectively. (**L** and **M**) Quantification of foci in muscle (L) ($n \geq 21$), (M) ($n \geq 21$). *T* test analysis with $^{**}P < 0.01$ and $^{***}P < 0.001$. See Supplemental Tables: 2, 3, and 4 for details and additional trials.

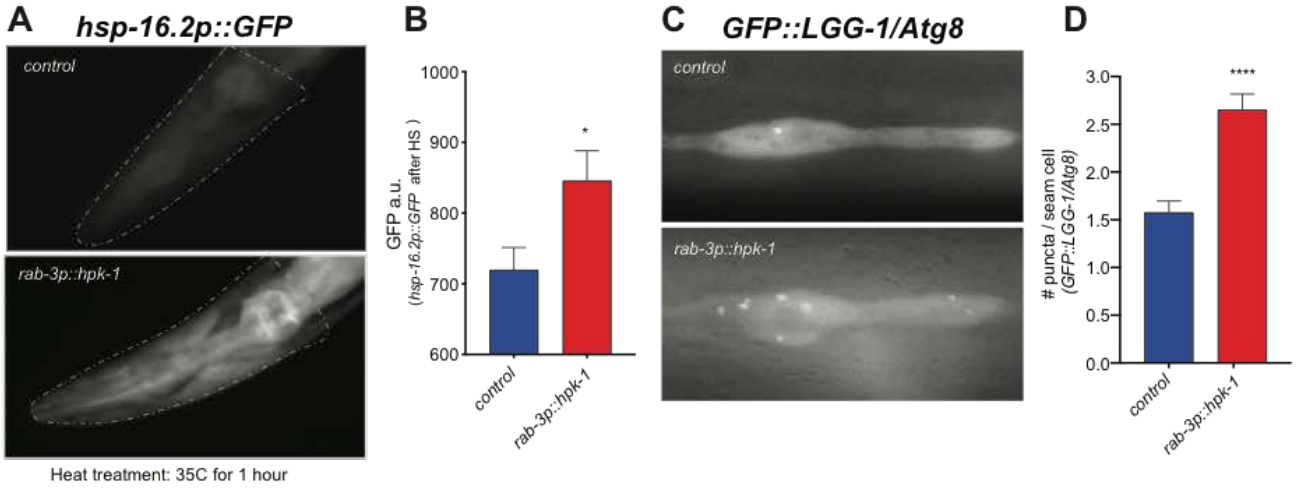

Fig 3. Neuronal HPK-1 induces the proteostatic network.

(A and **B)** Fluorescent micrographs (A) and fluorescent density quantification (B) of control and *rab-3p::hpk-1* of day 1 adult animals expressing *hsp-16.2::GFP* molecular chaperone reporter that were exposed to heat shock for 1 hour at 35°C ($n \geq 15$). **(C** and **D)** Fluorescent micrographs (C) and quantification (D) of puncta in seam cells of control and *rab-3p::hpk-1* of L4 stage animals expressing the *lgg-1p::GFP::LGG-1/Atg8* autophagosome reporter ($n \geq 43$). *T* test analysis with $^{*}P < 0.05$, $^{**}P < 0.01$, $^{***}P < 0.001$ and $^{****}P < 0.0001$. See Supplemental Tables 6 and 7 for details and additional trials.

Fig 4

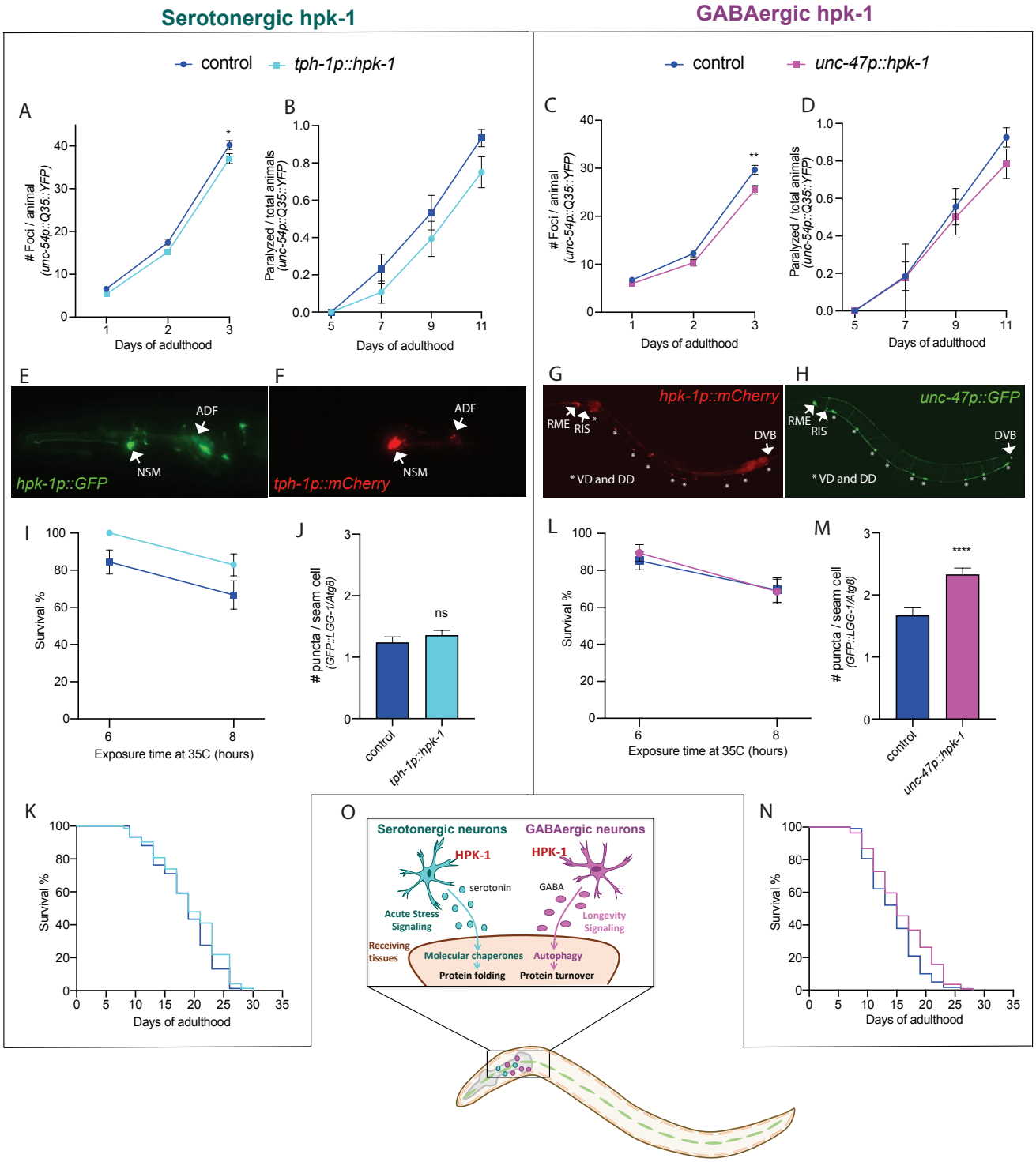
Serotonergic hpk-1
GABAergic hpk-1
control
tph-1p::hpk-1
unc-47p::hpk-1
A
B
C
D
Foci / animal (unc-54p::Q35::YFP)
Paralyzed / total animals (unc-54p::Q35::YFP)
Days of adulthood
E
F
G
H
ADF
NSM
hpk-1p::GFP
tph-1p::mCherry
hpk-1p::mCherry
unc-47p::GFP
RME
RIS
DVB
* VD and DD
I
J
L
M
Survival %
Exposure time at 35C (hours)
puncta / seam cell (GFP::LGG-1/Atg8)
ns
control
tph-1p::hpk-1
unc-47p::hpk-1
K
N
O
Serotonergic neurons
GABAergic neurons
HPK-1
serotonin
GABA
Acute Stress Signaling
Longevity Signaling
Receiving tissues
Molecular chaperones
Autophagy
Protein folding
Protein turnover

Fig 4. Serotonergic and GABAergic HPK-1 signaling regulate distinct adaptive responses to coordinate proteostasis, stress resistance, and longevity.

(A and **B)** Quantification of foci (A) and paralysis rate (B) of animals expressing *hpk-1* in serotonergic neurons (n≥17 for A and n≥28 for B). **(C** and **D)** Quantification of foci (C) and paralysis rate (D) of animals expressing *hpk-1* in GABAergic neurons (n≥19 for C and n≥27 for D). **(E** and **F)** Fluorescent micrographs of endogenous *hpk-1* expression in serotonergic neurons. **(G** and **H)** Fluorescent micrographs of endogenous *hpk-1* expression in GABAergic neurons. **(I)** Survival of serotonergic HPK-1 animals after heat shock (n≥32). **(J)** Quantification of autophagosomes in hypodermal cells of serotonergic HPK-1 animals (n≥80). **(K)** Lifespan of serotonergic HPK-1 (n≥76). **(L)** Survival of GABAergic HPK-1 animals after heat shock (n≥47). **(M)** Quantification of autophagosomes in hypodermal cells of GABAergic HPK-1 animals (n≥64). **(N)** Lifespan of GABAergic HPK-1 animals (n≥119). **(O)** Model diagram of serotonergic and GABAergic HPK-1 regulatory mechanism to mediate proteostasis and longevity. *T* test analysis with $^{*}P < 0.05$, $^{**}P < 0.01$ and $^{****}P < 0.0001$. See Supplemental Tables: 1, 2, 4, 5, and 7 for details and additional trials.

Supplementary Materials for

Neuroendocrine control of the proteostatic network by HPK-1 delays aging

Maria I. Lazaro-Pena, Carlos A. Diaz-Balzac, Ritika Das, and Andrew Samuelson*

* Corresponding author. Andrew_Samuelson@URMC.Rochester.edu

This PDF file includes:

- Materials and Methods
- Figs. S1 to S7
- Tables S1 to S8
- References

Materials and Methods

C. elegans strains and details

All strains were maintained at 20°C on standard NGM plates with OP50. For all experiments, animals were grown in 20x concentrated HT115 bacteria seeded on 6cm RNAi plates. Details on the strains, mutant alleles, and transgenic animals used in this study are listed below.

Strain name	Genotype
N2	*Wild type*
AVS392	*hpk-1(pk1393) X*
AVS543	*artEx41 [rab-3p::hpk-1::CFP + pCFJ90 (myo-2p::mCherry)]*
AVS609	*artEx43 [myo-3p::hpk-1 + pCFJ90 (myo-2p::mCherry)] line 1*
AVS614	*artEx48 [dpy-7p::hpk-1 + pCFJ90 (myo-2p::mCherry)] line 1*
AVS627	*artEx52 [ges-1p::hpk-1 + pCFJ90 (myo-2p::mCherry)] line 1*
AVS420	*hpk-1(pk1393) X; artEx41 [rab-3p::hpk-1::CFP + pCFJ90 (myo-2p::mCherry)]*
AVS602/CZ13799	*juIs76 [unc-25p::GFP + lin-15(+)] II*
AVS608	*hpk-1(pk1393); juIs76 [unc-25p::GFP + lin-15(+)] II*
AVS752	*artEx41 [rab-3p::hpk-1::CFP + pCFJ90 (myo-2p::mCherry)]; hpk-1(pk1393); juIs76 [unc-25p::GFP + lin-15(+)] II*
AVS832	*rmIs132 [unc-54p::Q35::YFP] I; artEx58 [rab-3p::hpk-1 + pCFJ90 (myo-2p::mCherry)] line 1*
AVS833	*rmIs132 [unc-54p::Q35::YFP] I; artEx59 [rab-3p::hpk-1 + pCFJ90 (myo-2p::mCherry)] line 2*
AVS834	*rmIs132 [unc-54p::Q35::YFP] I; artEx60 [rab-3p::hpk-1 + pCFJ90 (myo-2p::mCherry)] line 3*
AVS835	*rmIs132 [unc-54p::Q35::YFP] I; artEx61 [rab-3p::hpk-1 + pCFJ90 (myo-2p::mCherry)] line 4*
AVS562	*rmIs132 [unc-54p::Q35::YFP] I; artEx41 [rab-3p::hpk-1::CFP + pCFJ90 (myo-2p::mCherry)] line 5*
AVS563	*rmIs110 [F25B3.3p::Q40::YFP]; artEx41 [rab-3p::hpk-1::CFP + pCFJ90 (myo-2p::mCherry)] line 1*
AVS837	*rmIs110 [F25B3.3p::Q40::YFP]; artEx92 [rab-3p::hpk-1::CFP + pCFJ90 (myo-2p::mCherry)] line 2*
AVS838	*rmIs110 [F25B3.3p::Q40::YFP]; artEx93 [rab-3p::hpk-1::CFP + pCFJ90 (myo-2p::mCherry)] line 3*
AVS839	*rmIs110 [F25B3.3p::Q40::YFP]; artEx94 [rab-3p::hpk-1::CFP + pCFJ90 (myo-2p::mCherry)] line 4*
AVS214/HC196	*sid-1(qt9) V*
AVS265/TU3401	*sid-1(pk3321)V; uIs69 [unc-119p::sid-1; myo-2p::mCherry]V*
AVS540	*rmIs132 [unc-54p::Q35::YFP] I; sid-1(pk3321)V; uIs69[unc-119p::sid-1; myo-2p::mCherry]V*
AVS541	*rmIs110 [F25B3.3p::Q40::YFP]; sid-1(pk3321)V; uIs69[unc-119p::sid-1; myo-2p::mCherry]V*
AVS713	*rmIs132 [unc-54p::Q35::YFP] I; artEx41(rab-3p::hpk-1::CFP + pCFJ90 (myo-2p::mCherry)]; unc-31(e169)V*
AVS810	*rmIs132 [unc-54p::Q35::YFP] I; artEx41 [rab-3p::hpk-1::CFP + pCFJ90 (myo-2p::mCherry)]; unc-13(e51)I*
AVS84/TJ375	*gpIs1 [hsp-16.2p::GFP] IV*
AVS397	*gpIs1 [hsp-16.2p::GFP]; artEx35 [sur-5p::hpk-1::CFP +pCFJ90 (myo-2p::mCherry)]*
AVS399	*gpIs1 [hsp-16.2p::GFP]; artEx33 [rab-3p::hpk-1::CFP +pCFJ90 (myo-2p::mCherry)]*
AVS715	*artEx41 [rab-3p::hpk-1::CFP + pCFJ90 (myo-2p::mCherry)]; sqIs24 [rgef-1p::GFP::lgg-1 + unc-122p::RFP]*
AVS716	*artEx41 [rab-3p::hpk-1::CFP + pCFJ90 (myo-2p::mCherry)]; sqIs13 [lgg-1p::GFP::lgg-1 + odr-1p::RFP]*
AVS682	*artEx62 [tph-1p::hpk-1 + pCFJ90 (myo-2p::mCherry)] line 1; rmIs132 [unc-54p::Q35::YFP] I*
AVS683	*artEx63 [tph-1p::hpk-1 + pCFJ90 (myo-2p::mCherry)] line 2; rmIs132 [unc-54p::Q35::YFP] I*
AVS685	*artEx65 [unc-47p::hpk-1 + pCFJ90 (myo-2p::mCherry)] line 1; rmIs132 [unc-54p::Q35::YFP] I*
AVS686	*artEx66 [unc-47p::hpk-1 + pCFJ90 (myo-2p::mCherry)] line 2; rmIs132 [unc-54p::Q35::YFP] I*
AVS691	*artEx71 [eat-4p::hpk-1 + pCFJ90 (myo-2p::mCherry)] line 1; rmIs132 [unc-54p::Q35::YFP] I*
AVS692	*artEx72 [eat-4p::hpk-1 + pCFJ90 (myo-2p::mCherry)] line 2; rmIs132 [unc-54p::Q35::YFP] I*
AVS693	*artEx73 [cat-2p::hpk-1 + pCFJ90 (myo-2p::mCherry)] line 1; rmIs132 [unc-54p::Q35::YFP] I*
AVS694	*artEx74 [cat-2p::hpk-1 + pCFJ90 (myo-2p::mCherry)] line 2; rmIs132 [unc-54p::Q35::YFP] I*
AVS809	*artEx62 [tph-1p::hpk-1 + pCFJ90 (myo-2p::mCherry)] line 1; sqIs13 [lgg-1p::GFP::lgg-1 + odr-1p::RFP]*
AVS794	*artEx65 [unc-47p::hpk-1 + pCFJ90 (myo-2p::mCherry)] line 1; sqIs13 [lgg-1p::GFP::lgg-1 + odr-1p::RFP]*
AVS709	*artEx62 [tph-1p::hpk-1 + pCFJ90 (myo-2p::mCherry)] line 1*
AVS710	*artEx65 [unc-47p::hpk-1 + pCFJ90 (myo-2p::mCherry)] line 1*
AVS836	*artEx91 [hpk-1p::GFP + tph-1p::mCherry] line 1*
AVS757	*artEx87 [hpk-1p::mCherry + unc-47p::GFP] line 1*

Strains with both an AVS# and an external designation were generated in another laboratory. In these cases, an AVS# is assigned for internal record keeping and increased rigor and reproducibility purposes.

Generation of transgenic strains

To assemble tissue-specific constructs for overexpression experiments, the *hpk-1* cDNA was cloned under control of the following promoters: hypodermal *dpy-7p* (*1*), body wall muscle *myo-3p* (*2*), pan-neuronal *rab-3p* (*3*), dopaminergic neurons *cat-2p* (*4*), glutamatergic neurons *eat-4p* (*5*), serotonergic neurons *tph-1p* (*6*), and g-aminobutyric acid (GABA)ergic neurons *unc-47p* (*7*). All plasmids contained the *unc-54* 3'-UTR. These constructs for were injected at 5 ng/ml together with *myo-2p::mCherry* construct at 5 ng/ml as injection marker.

RNAi feeding

The *hpk-1* RNAi clone was originated from early copies of *E. coli* glycerol stocks of the comprehensive RNAi libraries generated in the Ahringer and Vidal laboratories. The control empty vector (L4440) and *hpk-1* RNAi colonies were grown overnight in Luria broth with 50 µg ml–1 ampicillin and then seeded onto 6cm RNAi agar plates containing 5 mM isopropylthiogalactoside (IPTG) to induce dsRNA expression overnight at room temperature. RNAi clones used in this study were verified by DNA sequencing and subsequent BLAST analysis to confirm their identity.

The nervous system of wild-type *C. elegans* is largely refractory to RNAi, as these cells do not express *sid-1*, which is necessary for dsRNA transport into neurons (*8-10*). Enhanced neuronal RNAi can be obtained by ectopic neuronal expression of *sid-1*(*11*). We crossed the *rgef-1p::Q40::YFP* reporter with *sid-1(pk3321);unc-119p::sid*-1 for neuronal downregulation experiments.

Lifespan analysis

Lifespan assays were performed essentially as described in: (*12, 13*). Briefly, animals were synchronized by egg prep bleaching followed by hatching in M9 solution at 20C overnight. The L1 animals were seeded onto 6cm plates with HT115 bacteria and allowed to develop at 20°C. At L4 stage, 2' fluoro– 5'deoxyuridine (FUDR) was added to a final concentration of 400 uM to prevent progeny production (defined as day 0 adulthood). Viability was scored every day or every other day as indicated in each figure. Prism 7 was used to for statistical analyses and the *P* values were calculated using long-rank (Mantel-Cox) method.

Thermotolerance assay

Survival assays at high temperature were conducted as previously described in (*14*). In brief, synchronized L1 animals were allowed to develop at 20°C; FUDR was added at the L4 stage to prevent progeny production. At day 1 adulthood, animals were moved to 35°C for a period of 6 and 8 hours. Animals were allowed to recover for 2 hours at 20°C, and viability was scored. Statistical testing between pairs of conditions for differences in the number of foci was performed using student's *t* test analysis.

Induction of *hsp-16.2p*::*GFP* after heat shock

The *hsp-16.2p*::*GFP* animals were heat shocked on day 1 of adulthood for 1 hour at 35°C and imaged after 4 hours of recovery. *I*mages were acquired using a Zeiss Axio Imager M2m microscope with AxioVision v4.8.2.0 software. The GFP a.u. values from the head and intestine of the animals were acquired using the area selection feature from

AxioVision software. Two independent trials with a minimum of 20 animals per experiment were performed.

Measurement of autophagosome formation using the *GFP::LGG-1/Atg8* reporter.
GFP::LGG-1/Atg8 foci formation was visualized as described in (*15*). Briefly, L4 stage and day 1 adult animals were raised on HT115 bacteria at 20°C and imaged using a Zeiss Axio Imager M2m microscope with AxioVision v4.8.2.0 software at 63X magnification. More than 40 seam cells from 15-20 different animals were scored for *GFP::LGG-1* puncta accumulation. Two independent trials with a minimum of 20 animals per experiment were performed.

Measurement of neurodegeneration in motor neurons
Animals carrying the *unc-25p::GFP* reporter strain to visualize VD and DD motor neurons were synchronized and allowed to developed at 20°C and FUDR was added at L4 stage to prevent progeny production. At L4, D2 and D9 of adulthood, animals were imaged in a Zeiss Axio Imager M2m microscope and the number of animals showing axonal breaks in the VD and DD motor neurons were scored. Axonal breaks were defined as an area of discontinued fluorescence in either the ventral or dorsal nerve cords.

Polyglutamine aggregation in neurons and locomotion analyses
The visualization and quantification of the progressive decline in proteostasis in the nervous system (specifically the nerve ring) was performed as described in (*16, 17*). In brief, synchronized *rgef-1p*::*polyQ40*::*YFP* L4 animals were treated with FUDR to prevent progeny production. Then, z stack images from the nerve ring were acquired using a Zeiss Axio Imager M2m microscope with AxioVision v4.8.2.0 software at 63X magnification. The fluorescent foci form compressed *z*-stack images from 20 animals per technical replicate were scored blind every other day from four to eight days of adulthood. To assess locomotion capacity, at day two of adulthood, 40 animals were transferred to a drop of 10ul of M9 solution and the number of body bends performed in a period of 30 seconds from each animal was scored (as described in (*17*)). Statistical testing between pairs of conditions for differences in the number of foci was performed using student's *t* test analysis.

Polyglutamine aggregation in muscle and paralysis analyses
The visualization and quantification of the progressive decline in proteostasis in muscle tissue was performed as described in (*17, 18*). Briefly, synchronized *unc-54p*::*polyQ35*::*YFP* L4 animals were treated with FUDR to prevent progeny production. Then, fluorescent foci from 20 animals per technical replicate were scored blind daily from days one to three of adulthood. To assess paralysis, at days 5,7,9 and 11 of adulthood, prodded animals that responded with head movement (and were therefore still alive) but no backward or repulsive motion were scored as paralyzed (as described in (*17*)). Statistical testing between pairs of conditions for differences in the number of foci was performed using student's *t* test analysis. Two to five independent transgenics lines were tested.

Aldicarb assay

The aldicarb assay was performed as described in (*19, 20*). Plates containing Aldicarb 1mM were prepared the day before the assay and stored at 4°C. Animals were synchronized by picking at L4 stage and placing them in a plate with HT115 bacteria. After 24 hours, one aldicarb plate per strain were brought out of 4°C and a small drop of OP50 was placed in the center of the plate a let dry for 30 minutes. Approximately 25 animals were placed on each plate, and the number of paralyzed animals were scored every hour up to 5 hours. The assay was performed at room temperature.

Exogenous 5-HT immobilization assay

Animals were synchronized by picking at L4 stage and placing them in a plate with HT115 bacteria. After 24 hours, serotonin (5-HT) was dissolved in M9 buffer to a 20mM concentration (*21*). Twenty worms were placed on a glass plate well with 400ul of 20mM serotonin for 10 minutes. The same number of control animals were placed in 400ul of M9 buffer. The locomotion of worms (mobilize or immobilized) was annotated at the following time points: 2, 4, 6, 8, and 10 minutes. The assay was performed at room temperature.

Statistical analyses

Graphpad PRISM7 software was used for all statistical analyses. Data were considered statistically significant when P value was higher than 0.05. In figures, asterisks denote statistical significance as (*, $P < 0.05$, **, $P < 0.001$, ****, $P < 0.0001$) as compared to appropriate controls. N number listed in figure legend indicates the number of one representative experiment among all biological trials.

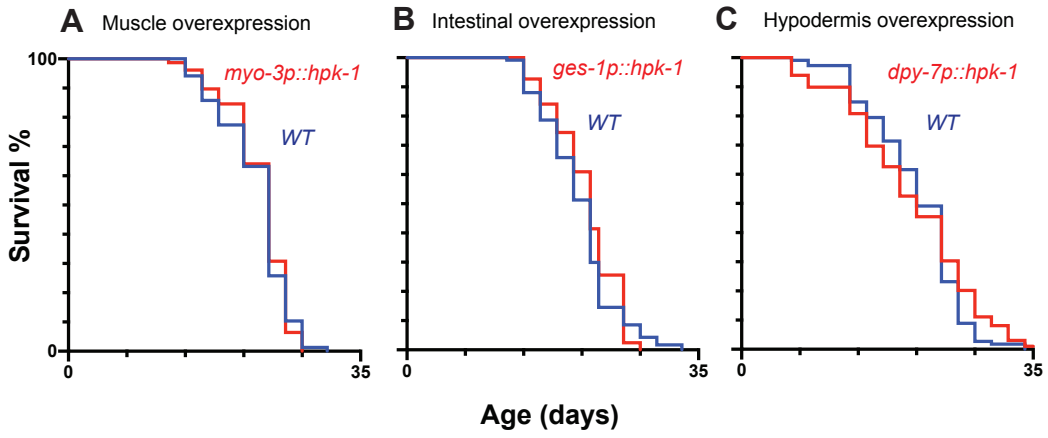

Figure S1. HPK-1 overexpression in muscle, intestine and hypodermis is not sufficient to increase lifespan. Survival curves of animals expressing *hpk-1* (red line) in the muscles (*myo-3p::hpk-1*) **(A)**, intestine (*ges-1p::hpk-1*) **(B)** and hypodermis (*dpy-7p::hpk-1*) **(C)**, compared with control non-transgenic siblings (blue line). Animals were maintained at 20°C ($n \geq 78$ for A, $n \geq 82$ for B and $n \geq 105$ for C). Lifespan graphs are representative of two biological replicates. See Supplemental Table 1 for details and additional trials.

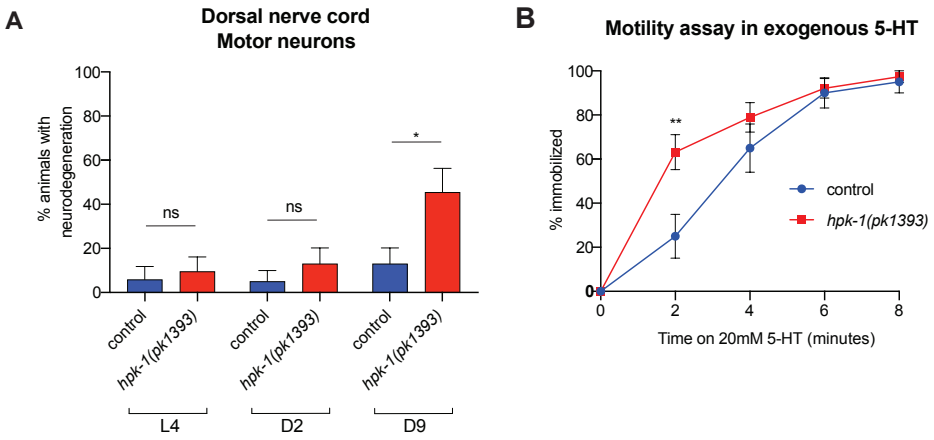

Figure S2. *hpk-1* loss of function induces DD motor neuron neurodegeneration and hypersensitivity to exogenous 5-HT immobilization. (A) Percentage of control and *hpk-1(pk1393)* animals with neurodegeneration in DD motor neurons ($n \geq 17$). **(B)** Percentage of immobilized control (blue) and *hpk-1(pk1393)* (red) of day 1 adult animals after eight hours of exposure to 20mM 5-HT ($n \geq 38$). *T* test analysis with $^*P < 0.05$. See Supplemental Tables 8 and 10 for details and additional trials.

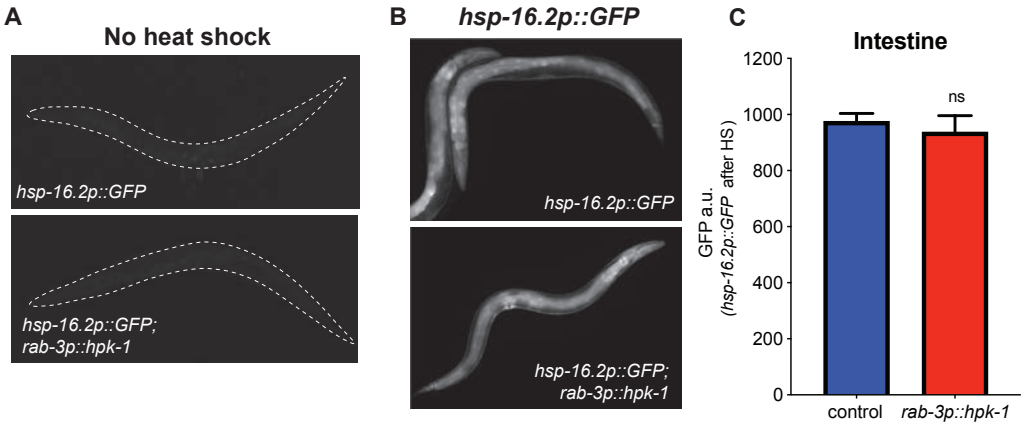

Figure S3. Neuronal HPK-1 does not hyper-induces molecular chaperones in the intestine. (A) Animals expressing *hsp-16.2p::GFP* in basal condition. **(B)** Animals expressing *hsp-16.2p::GFP* after heat shock treatment for 1hr at 35°C. **(C)** GFP densitometry quantification on the intestine of day 1 adults after heat treatment from *hsp-16.2p::GFP* expressing animals (n≥24). See Supplemental Table 6 for details and additional trials.

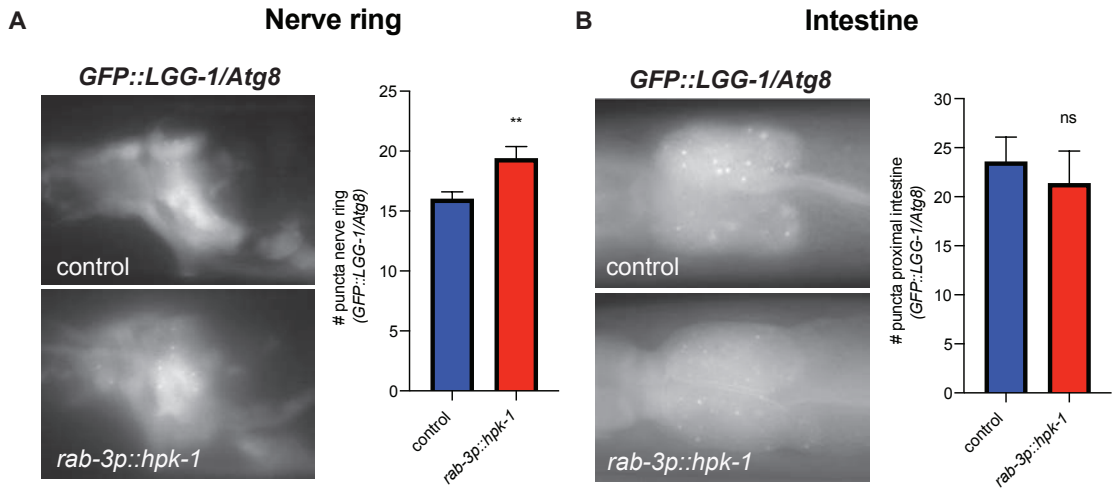

Figure S4. Neuronal overexpression of HPK-1 increases the number of autophagosomes in the nervous system, but do not changes autophagosome number in the intestine. (A) Fluorescent micrographs and quantification of puncta in the nerve ring of control and *rab-3p::hpk-1* of L4 stage animals expressing the *rgef-1p::GFP::LGG-1/Atg8* autophagosome reporter (n$\geq$21). (B) Fluorescent micrographs and quantification of puncta in proximal intestinal cells of control and *rab-3p::hpk-1* of L4 stage animals expressing the *lgg-1p::GFP::LGG-1/Atg8* autophagosome reporter (n$\geq$17). *T* test analysis with $^{**}P < 0.01$. See Supplemental Table 7 for details and additional trials.

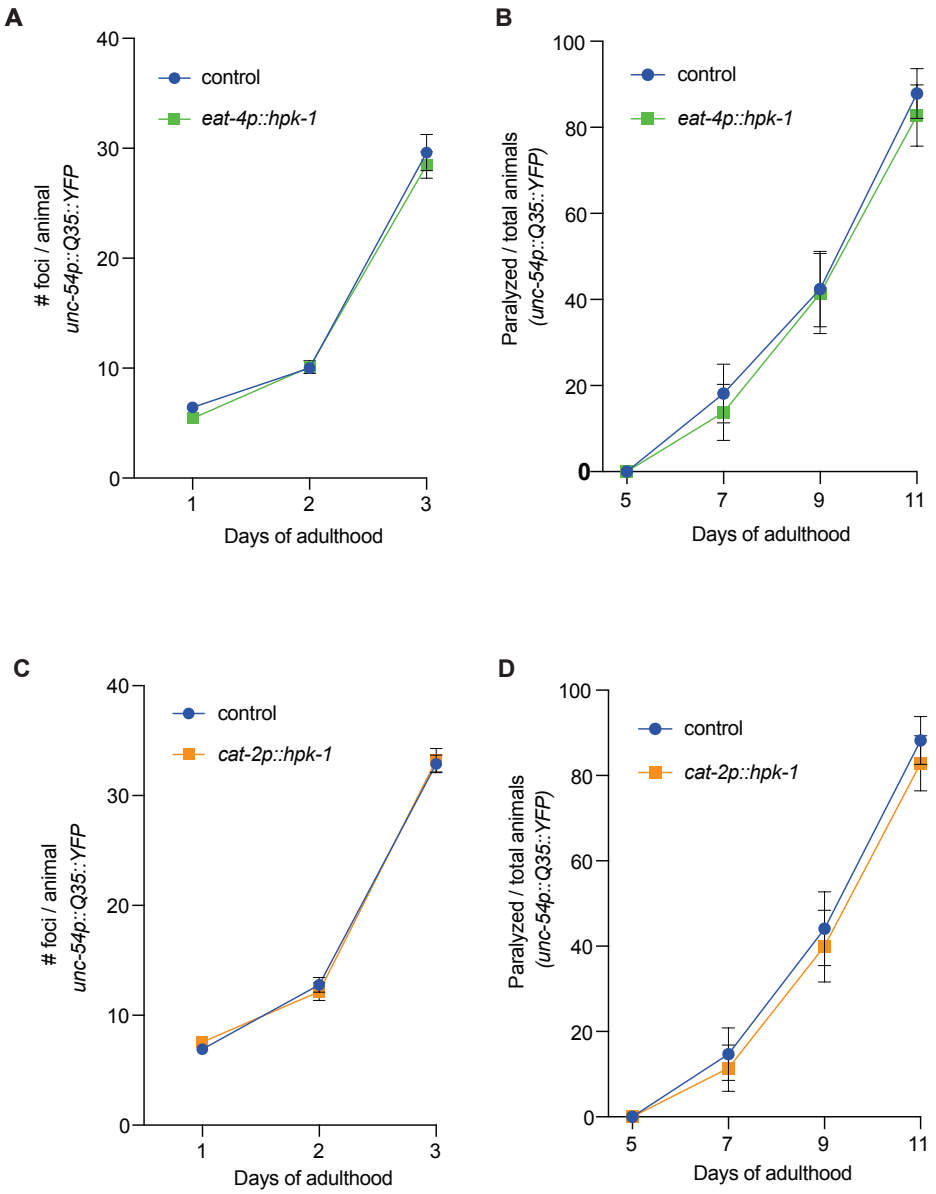

Figure S5. *hpk-1* expression in glutamatergic and dopaminergic neurons is not sufficient to prevent the decline in proteostasis. (A and **B)** Quantification of number of foci (A) and paralysis rate (B) of animals expressing *hpk-1* in the glutamatergic neurons (*eat-4p::hpk-1*; green line) and control non-transgenic siblings (blue line) ($n \geq 18$ for A and $n \geq 29$ for B). **(C** and **D)** Quantification of number of foci (C) and paralysis rate (D) of animals expressing *hpk-1* in the dopaminergic neurons (*cat-2p::hpk-1;* orange line) and control non-transgenic siblings (blue line) ($n \geq 16$ for C and $n \geq 34$ for D). See Supplemental Tables 2 and 4 for details and additional trials.

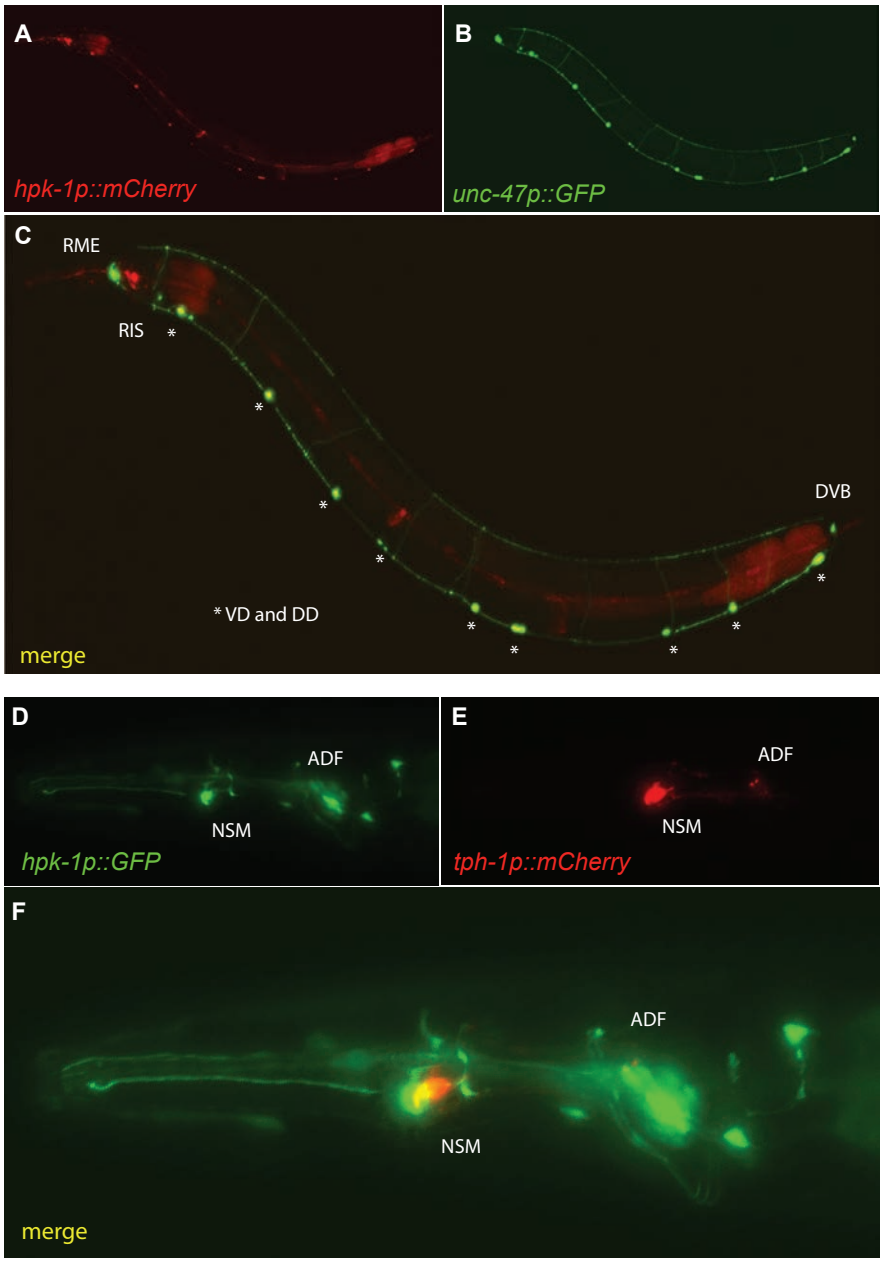

Figure S6. *hpk-1* is expressed in GABAergic and serotonergic neurons. Representative fluorescent micrographs of day 1 adult animals co-expressing *hpk-1p::mCherry* and *unc-47p::GFP* **(A-C)**; and *hpk-1p::GFP* and *tph-1p::mCherry* **(D-F)**.

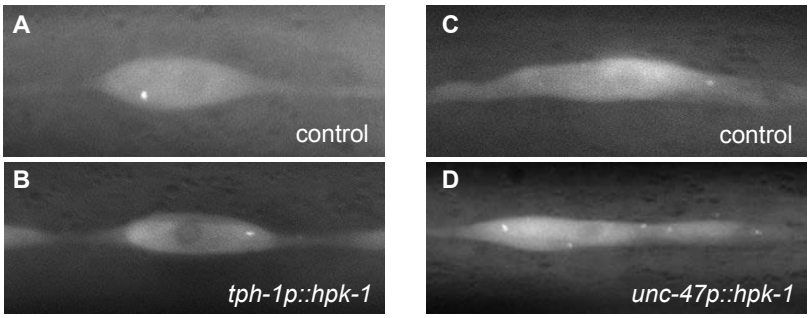

Figure S7. *hpk-1* expression in GABAergic neurons, but not in serotonergic neurons, induces autophagy activity in hypodermal seam cells. Representative fluorescent micrographs (from data in Figure 4J,M), showing autophagosome fluorescent puncta in seam cells of day 1 adult animals expressing *GFP::LGG-1/Atg8* autophagosome reporter with *hpk-1* expression in serotonergic (**A** and **B**) and GABAergic (**C** and **D**) neurons.

Table S1. Lifespan assays data of representative experiments in figures and additional trials.

Figure/ Trials	Strain / Genotype	Median Survival	Total animals (n number)	95% CI of ratio	*P* value compared to WT	Significance
Fig. 1A Trial 1	AVS543: control	18	175	0.6989 to 1.051	**n/a**	**n/a**
	AVS543: *artEx41 [rab-3p::hpk-1::CFP + pCFJ90 (myo-2p::mCherry)]*	21	195	0.6989 to 1.051	<0.0001	****
Fig. 1A Trial 2	AVS399: *gpIs1 [hsp-16.2p::GFP]*	22	264	0.7557 to 1.112	**n/a**	**n/a**
	AVS399*: gpIs1 [hsp-16.2p::GFP]; artEx33 [rab-3p::hpk-1::CFP +pCFJ90 (myo-2p::mCherry)]*	24	169	0.7557 to 1.112	<0.0001	****
Fig. 4K	AVS709: control	19	73	0.7253 to 1.379	**n/a**	**n/a**
	AVS709: *artEx62 [tph-1p::hpk-1 + pCFJ90 (myo-2p::mCherry)] line 1*	19	76	0.7253 to 1.379	0.1434	**ns**
Fig. 4N	AVS710: control	15	114	0.7735 to 1.293	**n/a**	**n/a**
	AVS710: *artEx65 [unc-47p::hpk-1 + pCFJ90 (myo-2p::mCherry)] line 1*	15	119	0.7735 to 1.293	0.0074	**
Fig. S1A	AVS609: control	24	175	0.7618 to 1.313	n/a	n/a
	AVS609: *artEx43 [myo-3p::hpk-1 + pCFJ90 (myo-2p::mCherry)] line 1*	24	195	0.7618 to 1.313	0.9304	ns
Fig. S1B	AVS614: control	21	99	0.7631 to 1.310	n/a	n/a
	AVS614: *artEx48 [dpy-7p::hpk-1 + pCFJ90 (myo-2p::mCherry)] line 1*	21	112	0.7631 to 1.310	0.9304	ns
Fig. S1B	AVS627: control	22	117	0.7541 to 1.326	n/a	n/a
	AVS627: *artEx52 [ges-1p::hpk-1 + pCFJ90 (myo-2p::mCherry)] line 1*	22	82	0.7541 to 1.326	0.3226	ns

Table S2. Polyglutamine aggregates data of representative experiments in figures and additional trials.

Figure/ Trials	Strain / Genotype	RNAi	Days of adulthood	#Foci/animal (mean)	Total cells (n number)	SEM	*P* value compared to control	Significance
Fig. 2B Line 1	AVS563: *rmIs110 [F25B3.3p::Q40::YFP]*	**n/a**	4	2.409	22	0.252	**n/a**	**n/a**
	AVS563: *rmIs110 [F25B3.3p::Q40::YFP]*	**n/a**	6	4.286	28	0.352	**n/a**	**n/a**
	AVS563: *rmIs110 [F25B3.3p::Q40::YFP]*	**n/a**	8	5.231	26	0.445	**n/a**	**n/a**
	AVS563: *rmIs110 [F25B3.3p::Q40::YFP]; artEx41 [rab-3p::hpk-1::CFP + pCFJ90 (myo-2p::mCherry)]*	**n/a**	4	2.13	23	0.297	0.4799	ns
	AVS563: *rmIs110 [F25B3.3p::Q40::YFP]; artEx41 [rab-3p::hpk-1::CFP + pCFJ90 (myo-2p::mCherry)]*	**n/a**	6	3.333	21	0.47	0.1042	ns
	AVS563: *rmIs110 [F25B3.3p::Q40::YFP]; artEx41 [rab-3p::hpk-1::CFP + pCFJ90 (myo-2p::mCherry)]*	**n/a**	8	4.125	24	0.41	0.0751	ns
Fig. 2B Lines 2, 3, 4	AVS837: *rmIs110 [F25B3.3p::Q40::YFP]*	**n/a**	8	8.4	20	0.4554	n/a	n/a
	AVS837: *rmIs110 [F25B3.3p::Q40::YFP]; artEx92 [rab-3p::hpk-1::CFP + pCFJ90 (myo-2p::mCherry)]*	**n/a**	8	5.95	20	0.3118	<0.0001	****
	AVS838: *rmIs110 [F25B3.3p::Q40::YFP]*	**n/a**	8	6.8	20	0.3811	n/a	n/a
	AVS838*rmIs110 [F25B3.3p::Q40::YFP]; artEx93 [rab-3p::hpk-1::CFP + pCFJ90 (myo-2p::mCherry)]*	**n/a**	8	6.2	20	0.2865	0.216	ns

	AVS839: *rmIs110 [F25B3.3p::Q40::YFP]*	**n/a**	8	6.7	20	0.3411	n/a	n/a
	AVS839: *rmIs110 [F25B3.3p::Q40::YFP]; artEx94 [rab-3p::hpk-1::CFP + pCFJ90 (myo-2p::mCherry)]*	**n/a**	8	4.65	20	0.4122	0.0005	***
Fig. 2D	AVS541: *rmIs110 [F25B3.3p::Q40::YFP]; sid-1(pk3321)V; uIs69[unc-119p::sid-1; myo-2p::mCherry]V*	*empty vector*	4	3.13	23	0.29	n/a	n/a
	AVS541: *rmIs110 [F25B3.3p::Q40::YFP]; sid-1(pk3321)V; uIs69[unc-119p::sid-1; myo-2p::mCherry]V*	*empty vector*	6	4.042	24	0.259	n/a	n/a
	AVS541: *rmIs110 [F25B3.3p::Q40::YFP]; sid-1(pk3321)V; uIs69[unc-119p::sid-1; myo-2p::mCherry]V*	*empty vector*	8	5.565	23	0.407	n/a	n/a
	AVS541: *rmIs110 [F25B3.3p::Q40::YFP]; sid-1(pk3321)V; uIs69[unc-119p::sid-1; myo-2p::mCherry]V*	*empty vector*	10	7.545	22	0.487	n/a	n/a
	AVS541: *rmIs110 [F25B3.3p::Q40::YFP]; sid-1(pk3321)V; uIs69[unc-119p::sid-1; myo-2p::mCherry]V*	*hpk-1*	4	3.238	21	0.292	0.7953	ns
	AVS541: *rmIs110 [F25B3.3p::Q40::YFP]; sid-1(pk3321)V; uIs69[unc-119p::sid-1; myo-2p::mCherry]V*	*hpk-1*	6	6.12	23	0.35	<0.0001	****
	AVS541: *rmIs110 [F25B3.3p::Q40::YFP]; sid-1(pk3321)V; uIs69[unc-119p::sid-1; myo-2p::mCherry]V*	*hpk-1*	8	7.875	24	0.687	0.0064	**
	AVS541: *rmIs110 [F25B3.3p::Q40::YFP]; sid-1(pk3321)V; uIs69[unc-119p::sid-1; myo-2p::mCherry]V*	*hpk-1*	10	10.11	19	0.772	0.0064	**
Fig. 2G Line 1	AVS832: *rmIs132 [unc-54p::Q35::YFP] I*	n/a	1	13.43	28	0.45	n/a	n/a
	AVS832: *rmIs132 [unc-54p::Q35::YFP] I*	n/a	2	16.62	21	0.95	n/a	n/a
	AVS832: *rmIs132 [unc-54p::Q35::YFP] I*	n/a	3	26	18	1.15	n/a	n/a
	AVS832: *rmIs132 [unc-54p::Q35::YFP] I; artEx58 [rab-3p::hpk-1::CFP + pCFJ90 (myo-2p::mCherry)]*	n/a	1	11.73	22	0.4798	0.013	*
	AVS832: *rmIs132 [unc-54p::Q35::YFP] I; artEx58 [rab-3p::hpk-1::CFP + pCFJ90 (myo-2p::mCherry)]*	n/a	2	14.11	19	0.5181	0.0303	*
	AVS832: *rmIs132 [unc-54p::Q35::YFP] I; artEx58 [rab-3p::hpk-1::CFP + pCFJ90 (myo-2p::mCherry)]*	n/a	3	21.29	24	0.9178	0.0024	**
Fig. 2G Line 2	AVS833: *rmIs132 [unc-54p::Q35::YFP] I*	n/a	1	12.19	21	0.646	n/a	n/a
	AVS833: *rmIs132 [unc-54p::Q35::YFP] I*	n/a	2	22.18	11	1.102	n/a	n/a
	AVS833: *rmIs132 [unc-54p::Q35::YFP] I*	n/a	3	35	18	1.576	n/a	n/a
	AVS833: *rmIs132 [unc-54p::Q35::YFP] I; artEx59 [rab-3p::hpk-1::CFP + pCFJ90 (myo-2p::mCherry)]*	n/a	1	11.05	20	0.59	0.2017	ns
	AVS833: *rmIs132 [unc-54p::Q35::YFP] I; artEx59 [rab-3p::hpk-1::CFP + pCFJ90 (myo-2p::mCherry)]*	n/a	2	16.16	19	0.76	<0.0001	****
	AVS833: *rmIs132 [unc-54p::Q35::YFP] I; artEx59 [rab-3p::hpk-1::CFP + pCFJ90 (myo-2p::mCherry)]*	n/a	3	30.63	24	1.17	0.0282	*
Fig. 2G Line 3	AVS834: *rmIs132 [unc-54p::Q35::YFP] I*	n/a	1	12.91	22	0.75	n/a	n/a
	AVS834: *rmIs132 [unc-54p::Q35::YFP] I*	n/a	2	19.83	23	0.86	n/a	n/a
	AVS834: *rmIs132 [unc-54p::Q35::YFP] I*	n/a	3	28	21	1.26	n/a	n/a
	AVS834: *rmIs132 [unc-54p::Q35::YFP] I; artEx60 [rab-3p::hpk-1::CFP + pCFJ90 (myo-2p::mCherry)]*	n/a	1	10.5	26	0.54	0.0105	*
	AVS834: *rmIs132 [unc-54p::Q35::YFP] I; artEx60 [rab-3p::hpk-1::CFP + pCFJ90 (myo-2p::mCherry)]*	n/a	2	16.12	26	0.69	0.0014	**

	AVS834: *rmIs132 [unc-54p::Q35::YFP] I; artEx60 [rab-3p::hpk-1::CFP + pCFJ90 (myo-2p::mCherry)]*	n/a	3	20.06	31	0.81	<0.0001	****
Fig. 2G Line 4	AVS835: *rmIs132 [unc-54p::Q35::YFP] I*	n/a	1	12.14	21	0.48	n/a	n/a
	AVS835: *rmIs132 [unc-54p::Q35::YFP] I*	n/a	2	20.78	23	0.8	n/a	n/a
	AVS835: *rmIs132 [unc-54p::Q35::YFP] I*	n/a	3	26.79	19	1	n/a	n/a
	AVS835: *rmIs132 [unc-54p::Q35::YFP] I; artEx61 [rab-3p::hpk-1::CFP + pCFJ90 (myo-2p::mCherry)]*	n/a	1	8.593	27	0.507	<0.0001	****
	AVS835: *rmIs132 [unc-54p::Q35::YFP] I; artEx61 [rab-3p::hpk-1::CFP + pCFJ90 (myo-2p::mCherry)]*	n/a	2	16.47	36	0.455	<0.0001	****
	AVS835: *rmIs132 [unc-54p::Q35::YFP] I; artEx61 [rab-3p::hpk-1::CFP + pCFJ90 (myo-2p::mCherry)]*	n/a	3	21.58	33	0.903	0.0005	***
Fig. 2G Line 5	AVS562: *rmIs132 [unc-54p::Q35::YFP] I*	n/a	1	7.185	27	0.453	n/a	n/a
	AVS562: *rmIs132 [unc-54p::Q35::YFP] I*	n/a	2	15.16	32	0.775	n/a	n/a
	AVS562: *rmIs132 [unc-54p::Q35::YFP] I*	n/a	3	28.05	39	0.99	n/a	n/a
	AVS562: *rmIs132 [unc-54p::Q35::YFP] I*	n/a	4	41	25	1.268	n/a	n/a
	AVS562: *rmIs132 [unc-54p::Q35::YFP] I; artEx41 [rab-3p::hpk-1::CFP + pCFJ90 (myo-2p::mCherry)]*	n/a	1	5.409	22	0.495	0.0111	*
	AVS562: *rmIs132 [unc-54p::Q35::YFP] I; artEx41 [rab-3p::hpk-1::CFP + pCFJ90 (myo-2p::mCherry)]*	n/a	2	11.05	20	0.956	0.0017	**
	AVS562: *rmIs132 [unc-54p::Q35::YFP] I; artEx41 [rab-3p::hpk-1::CFP + pCFJ90 (myo-2p::mCherry)]*	n/a	3	21.14	21	0.996	<0.0001	****
	AVS562: *rmIs132 [unc-54p::Q35::YFP] I; artEx41 [rab-3p::hpk-1::CFP + pCFJ90 (myo-2p::mCherry)]*	n/a	4	32.95	21	1.702	0.0004	***
Fig. 2I	AVS540: *rmIs132 [unc-54p::Q35::YFP] I; sid-1(pk3321)V; uIs69[unc-119p::sid-1; myo-2p::mCherry]V*	*empty vector*	1	6.091	22	0.446	n/a	n/a
	AVS540: *rmIs132 [unc-54p::Q35::YFP] I; sid-1(pk3321)V; uIs69[unc-119p::sid-1; myo-2p::mCherry]V*	*empty vector*	2	8.125	24	0.368	n/a	n/a
	AVS540: *rmIs132 [unc-54p::Q35::YFP] I; sid-1(pk3321)V; uIs69[unc-119p::sid-1; myo-2p::mCherry]V*	*empty vector*	3	18.64	25	0.781	n/a	n/a
	AVS540: *rmIs132 [unc-54p::Q35::YFP] I; sid-1(pk3321)V; uIs69[unc-119p::sid-1; myo-2p::mCherry]V*	*empty vector*	4	32.48	29	1.105	n/a	n/a
	AVS540: *rmIs132 [unc-54p::Q35::YFP] I; sid-1(pk3321)V; uIs69[unc-119p::sid-1; myo-2p::mCherry]V*	*hpk-1*	1	7.609	23	0.434	0.0189	*
	AVS540: *rmIs132 [unc-54p::Q35::YFP] I; sid-1(pk3321)V; uIs69[unc-119p::sid-1; myo-2p::mCherry]V*	*hpk-1*	2	12.95	22	0.64	<0.0001	****
	AVS540: *rmIs132 [unc-54p::Q35::YFP] I; sid-1(pk3321)V; uIs69[unc-119p::sid-1; myo-2p::mCherry]V*	*hpk-1*	3	27.12	26	1.209	<0.0001	****
	AVS540: *rmIs132 [unc-54p::Q35::YFP] I; sid-1(pk3321)V; uIs69[unc-119p::sid-1; myo-2p::mCherry]V*	*hpk-1*	4	45.32	28	1.04	<0.0001	****
Fig. 2L,M	AVS562: *rmIs132 [unc-54p::Q35::YFP] I*	n/a	3	28.05	39	0.9898	n/a	n/a
	AVS562: *rmIs132 [unc-54p::Q35::YFP] I; artEx41 [rab-3p::hpk-1::CFP + pCFJ90 (myo-2p::mCherry)]*	n/a	3	21.14	21	0.9959	n/a	n/a
	AVS713: *rmIs132 [unc-54p::Q35::YFP] I; unc-31(e169)V*	n/a	3	21.52	58	0.6527	n/a	n/a
	AVS713: *rmIs132 [unc-54p::Q35::YFP] I; artEx41(rab-3p::hpk-1::CFP + pCFJ90 (myo-2p::mCherry)]; unc-31(e169)V*	n/a	3	18.02	50	0.5859	Compared to AVS713 control: 0.0001	***

	AVS810*rmIs132 [unc-54p::Q35::YFP] I; unc-13(e51)I*	n/a	3	57.81	26	1.098	n/a	n/a
	AVS810*rmIs132 [unc-54p::Q35::YFP] I; artEx41 [rab-3p::hpk-1::CFP + pCFJ90 (myo-2p::mCherry)]; unc-13(e51)I*	n/a	3	58.68	25	1.408	Compared to AVS810 control: 0.6258	ns
Fig. 4A Line 1	AVS682: *rmIs132 [unc-54p::Q35::YFP] I*	n/a	1	6.563	32	0.301	n/a	n/a
	AVS682: *rmIs132 [unc-54p::Q35::YFP] I*	n/a	2	17.43	30	0.7786	n/a	n/a
	AVS682: *rmIs132 [unc-54p::Q35::YFP] I*	n/a	3	40.23	26	1.017	n/a	n/a
	AVS682: *artEx62 [tph-1p::hpk-1 + pCFJ90 (myo-2p::mCherry)] line 1; rmIs132 [unc-54p::Q35::YFP] I*	n/a	1	5.333	21	0.252	0.0056	**
	AVS682: *artEx62 [tph-1p::hpk-1 + pCFJ90 (myo-2p::mCherry)] line 1; rmIs132 [unc-54p::Q35::YFP] I*	n/a	2	15.24	25	0.609	0.0359	*
	AVS682: *artEx62 [tph-1p::hpk-1 + pCFJ90 (myo-2p::mCherry)] line 1; rmIs132 [unc-54p::Q35::YFP] I*	n/a	3	37.06	17	1.152	0.0494	*
Fig. 4A Line 2	AVS683: *rmIs132 [unc-54p::Q35::YFP] I*	n/a	3	31.43	21	1.245	n/a	n/a
	AVS683: *artEx63 [tph-1p::hpk-1 + pCFJ90 (myo-2p::mCherry)] line 1; rmIs132 [unc-54p::Q35::YFP] I*	n/a	3	26.29	24	1.182	0.0046	**
Fig. 4C Line 1	AVS685: *rmIs132 [unc-54p::Q35::YFP] I*	n/a	1	6.737	19	0.3734	n/a	n/a
	AVS685: *rmIs132 [unc-54p::Q35::YFP] I*	n/a	2	12.26	19	0.696	n/a	n/a
	AVS685: *rmIs132 [unc-54p::Q35::YFP] I*	n/a	3	29.67	21	0.9394	n/a	n/a
	AVS685: *artEx65 [unc-47p::hpk-1 + pCFJ90 (myo-2p::mCherry)] line 1; rmIs132 [unc-54p::Q35::YFP] I*	n/a	1	6	25	0.2449	0.0937	ns
	AVS685: *artEx65 [unc-47p::hpk-1 + pCFJ90 (myo-2p::mCherry)] line 1; rmIs132 [unc-54p::Q35::YFP] I*	n/a	2	10.32	25	0.7158	0.064	ns
	AVS685: *artEx65 [unc-47p::hpk-1 + pCFJ90 (myo-2p::mCherry)] line 1; rmIs132 [unc-54p::Q35::YFP] I*	n/a	3	25.5	26	0.8931	0.0026	**
Fig. 4C Line 2	AVS686: *rmIs132 [unc-54p::Q35::YFP] I*	n/a	3	37.32	22	1.223	n/a	n/a
	AVS686: *artEx66 [unc-47p::hpk-1 + pCFJ90 (myo-2p::mCherry)] line 1; rmIs132 [unc-54p::Q35::YFP] I*	n/a	3	33.32	22	1.058	0.0175	*
Fig. S5A Line 1	AVS691: *rmIs132 [unc-54p::Q35::YFP] I*	n/a	1	6.44	25	0.2242	n/a	n/a
	AVS691: *rmIs132 [unc-54p::Q35::YFP] I*	n/a	2	10	32	0.4283	n/a	n/a
	AVS691: *rmIs132 [unc-54p::Q35::YFP] I*	n/a	3	29.6	20	1.663	n/a	n/a
	AVS691: *artEx71 [eat-4p::hpk-1 + pCFJ90 (myo-2p::mCherry)] line 1; rmIs132 [unc-54p::Q35::YFP] I*	n/a	1	5.444	18	0.2826	0.0079	**
	AVS691: *artEx71 [eat-4p::hpk-1 + pCFJ90 (myo-2p::mCherry)] line 1; rmIs132 [unc-54p::Q35::YFP] I*	n/a	2	10.1	21	0.5811	0.8935	ns
	AVS691: *artEx71 [eat-4p::hpk-1 + pCFJ90 (myo-2p::mCherry)] line 1; rmIs132 [unc-54p::Q35::YFP] I*	n/a	3	28.48	23	1.204	0.5812	ns
Fig. S5A Line 2	AVS692: *rmIs132 [unc-54p::Q35::YFP] I*	n/a	3	23.73	22	1.273	n/a	n/a
	AVS692: *artEx72 [eat-4p::hpk-1 + pCFJ90 (myo-2p::mCherry)] line 1; rmIs132 [unc-54p::Q35::YFP] I*	n/a	3	22.64	22	1.118	0.523	ns
Fig. S5C Line 1	AVS693: *rmIs132 [unc-54p::Q35::YFP] I*	n/a	1	6.906	36	0.1871	n/a	n/a

	AVS693: *rmIs132 [unc-54p::Q35::YFP] I*	n/a	2	12.77	26	0.6801	n/a	n/a
	AVS693: *rmIs132 [unc-54p::Q35::YFP] I*	n/a	3	32.88	33	0.7986	n/a	n/a
	AVS693: *artEx73 [cat-2p::hpk-1 + pCFJ90 (myo-2p::mCherry)] line 1; rmIs132 [unc-54p::Q35::YFP] I*	n/a	1	7.563	16	0.3648	0.0816	ns
	AVS693: *artEx73 [cat-2p::hpk-1 + pCFJ90 (myo-2p::mCherry)] line 1; rmIs132 [unc-54p::Q35::YFP] I*	n/a	2	12.15	20	0.8088	0.5587	ns
	AVS693: *artEx73 [cat-2p::hpk-1 + pCFJ90 (myo-2p::mCherry)] line 1; rmIs132 [unc-54p::Q35::YFP] I*	n/a	3	33.21	24	1.07	0.8019	ns
Fig. S5C Line 2	AVS694: *rmIs132 [unc-54p::Q35::YFP] I*	n/a	3	22.64	22	1.118	n/a	n/a
	AVS694: *artEx74 [cat-2p::hpk-1 + pCFJ90 (myo-2p::mCherry)] line 1; rmIs132 [unc-54p::Q35::YFP] I*	n/a	3	23.73	22	1.273	0.574	ns

Table S3. Body bends assay data.

Figure/ Trials	Strain / Genotype	RNAi	Body bends mean (30 seconds)	Total animals (n number)	SEM	*P* value compared to control	Significance
Fig. 1B	N2: *wild type*	n/a	48.72	40	0.7938	n/a	n/a
	AVS392: *hpk-1(pk1393)*	n/a	27.35	41	1.047	<0.0001	****
	AVS420: *hpk-1(pk1393) X; artEx41 [rab-3p::hpk-1::CFP + pCFJ90 (myo-2p::mCherry)]*	n/a	36.22	50	1.323	Compared to *hpk-1(pk1393):* <0.0001	****
Fig. 2C	AVS563: *rmIs110 [F25B3.3p::Q40::YFP]*	n/a	12.54	37	1.195	n/a	n/a
	AVS563: *rmIs110 [F25B3.3p::Q40::YFP]; artEx41 [rab-3p::hpk-1::CFP + pCFJ90 (myo-2p::mCherry)]*	n/a	17.69	36	0.9879	0.0014	**
Fig. 2E	AVS541: *rmIs110 [F25B3.3p::Q40::YFP]; sid-1(pk3321)V; uIs69[unc-119p::sid-1; myo-2p::mCherry]V*	*empty vector*	25.5	40	1.056	n/a	n/a
	AVS541: *rmIs110 [F25B3.3p::Q40::YFP]; sid-1(pk3321)V; uIs69[unc-119p::sid-1; myo-2p::mCherry]V*	*hpk-1*	19.69	39	0.8033	<0.0001	****

Table S4. Paralysis assay data of representative experiments in figures and additional trials.

Figure/ Trials	Strain / Genotype	RNAi	Days of adulthood	% of paralyzed animals	Total cells (n number)	SEM	*P* value compared to control	Significance
Fig. 2H Line 1	AVS832: *rmIs132 [unc-54p::Q35::YFP] I*	n/a	5	0%	27	0	**n/a**	**n/a**
	AVS832: *rmIs132 [unc-54p::Q35::YFP] I*	n/a	7	11%	27	0.06163	**n/a**	**n/a**
	AVS832: *rmIs132 [unc-54p::Q35::YFP] I*	n/a	9	33%	27	0.09245	**n/a**	**n/a**
	AVS832: *rmIs132 [unc-54p::Q35::YFP] I*	n/a	11	56%	27	0.09745	**n/a**	**n/a**
	AVS832: *rmIs132 [unc-54p::Q35::YFP] I*	n/a	13	81%	27	0.07618	**n/a**	**n/a**
	AVS832: *rmIs132 [unc-54p::Q35::YFP] I; artEx58 [rab-3p::hpk-1::CFP + pCFJ90 (myo-2p::mCherry)]*	n/a	5	0%	23	0	**n/a**	**n/a**
	AVS832: *rmIs132 [unc-54p::Q35::YFP] I; artEx58 [rab-3p::hpk-1::CFP + pCFJ90 (myo-2p::mCherry)]*	n/a	7	0%	23	0	0.1032	ns
	AVS832: *rmIs132 [unc-54p::Q35::YFP] I; artEx58 [rab-3p::hpk-1::CFP + pCFJ90 (myo-2p::mCherry)]*	n/a	9	17%	23	0.08081	0.2081	ns

	AVS832: *rmIs132 [unc-54p::Q35::YFP] I; artEx58 [rab-3p::hpk-1::CFP + pCFJ90 (myo-2p::mCherry)]*	n/a	11	43%	23	0.1057	0.405	ns
	AVS832: *rmIs132 [unc-54p::Q35::YFP] I; artEx58 [rab-3p::hpk-1::CFP + pCFJ90 (myo-2p::mCherry)]*	n/a	13	61%	23	0.1041	0.11	ns
Fig. 2H Line 2	AVS833: *rmIs132 [unc-54p::Q35::YFP] I*	n/a	5	0%	28	0	n/a	n/a
	AVS833: *rmIs132 [unc-54p::Q35::YFP] I*	n/a	7	21%	28	0.07897	n/a	n/a
	AVS833: *rmIs132 [unc-54p::Q35::YFP] I*	n/a	9	43%	28	0.09524	n/a	n/a
	AVS833: *rmIs132 [unc-54p::Q35::YFP] I*	n/a	11	79%	28	0.07897	n/a	n/a
	AVS833: *rmIs132 [unc-54p::Q35::YFP] I*	n/a	13	89%	28	0.05952	n/a	n/a
	AVS833: *rmIs132 [unc-54p::Q35::YFP] I; artEx59 [rab-3p::hpk-1::CFP + pCFJ90 (myo-2p::mCherry)]*	n/a	5	0%	20	0	n/a	n/a
	AVS833: *rmIs132 [unc-54p::Q35::YFP] I; artEx59 [rab-3p::hpk-1::CFP + pCFJ90 (myo-2p::mCherry)]*	n/a	7	5%	20	0.05	0.1166	ns
	AVS833: *rmIs132 [unc-54p::Q35::YFP] I; artEx59 [rab-3p::hpk-1::CFP + pCFJ90 (myo-2p::mCherry)]*	n/a	9	30%	20	0.1051	0.3751	ns
	AVS833: *rmIs132 [unc-54p::Q35::YFP] I; artEx59 [rab-3p::hpk-1::CFP + pCFJ90 (myo-2p::mCherry)]*	n/a	11	65%	20	0.1094	0.307	ns
	AVS833: *rmIs132 [unc-54p::Q35::YFP] I; artEx59 [rab-3p::hpk-1::CFP + pCFJ90 (myo-2p::mCherry)]*	n/a	13	80%	20	0.09177	0.3796	ns
Fig. 2H Line 3	AVS834: *rmIs132 [unc-54p::Q35::YFP] I*	n/a	5	0%	28	0	n/a	n/a
	AVS834: *rmIs132 [unc-54p::Q35::YFP] I*	n/a	7	3%	28	0.03571	n/a	n/a
	AVS834: *rmIs132 [unc-54p::Q35::YFP] I*	n/a	9	3%	28	0.03571	n/a	n/a
	AVS834: *rmIs132 [unc-54p::Q35::YFP] I*	n/a	11	39%	28	0.09399	n/a	n/a
	AVS834: *rmIs132 [unc-54p::Q35::YFP] I*	n/a	13	60%	28	0.09399	n/a	n/a
	AVS834: *rmIs132 [unc-54p::Q35::YFP] I; artEx60 [rab-3p::hpk-1::CFP + pCFJ90 (myo-2p::mCherry)]*	n/a	5	0%	22	0	n/a	n/a
	AVS834: *rmIs132 [unc-54p::Q35::YFP] I; artEx60 [rab-3p::hpk-1::CFP + pCFJ90 (myo-2p::mCherry)]*	n/a	7	5%	22	0.04545	0.8649	ns
	AVS834: *rmIs132 [unc-54p::Q35::YFP] I; artEx60 [rab-3p::hpk-1::CFP + pCFJ90 (myo-2p::mCherry)]*	n/a	9	5%	22	0.04545	0.8649	ns
	AVS834: *rmIs132 [unc-54p::Q35::YFP] I; artEx60 [rab-3p::hpk-1::CFP + pCFJ90 (myo-2p::mCherry)]*	n/a	11	23%	22	0.09145	0.2209	ns
	AVS834: *rmIs132 [unc-54p::Q35::YFP] I; artEx60 [rab-3p::hpk-1::CFP + pCFJ90 (myo-2p::mCherry)]*	n/a	13	41%	22	0.1073	0.1708	ns
Fig. 2H Line 4	AVS835: *rmIs132 [unc-54p::Q35::YFP] I*	n/a	5	0%	25	0	n/a	n/a
	AVS835: *rmIs132 [unc-54p::Q35::YFP] I*	n/a	7	0%	25	0	n/a	n/a
	AVS835: *rmIs132 [unc-54p::Q35::YFP] I*	n/a	9	20%	25	0.8165	n/a	n/a
	AVS835: *rmIs132 [unc-54p::Q35::YFP] I*	n/a	11	60%	25	0.1	n/a	n/a
	AVS835: *rmIs132 [unc-54p::Q35::YFP] I*	n/a	13	60%	25	0.1	n/a	n/a
	AVS835: *rmIs132 [unc-54p::Q35::YFP] I; artEx61 [rab-3p::hpk-1::CFP + pCFJ90 (myo-2p::mCherry)]*	n/a	5	0%	24	0	n/a	n/a

	AVS835: *rmIs132 [unc-54p::Q35::YFP] I; artEx61 [rab-3p::hpk-1::CFP + pCFJ90 (myo-2p::mCherry)]*	n/a	7	0%	24	0	n/a	n/a
	AVS835: *rmIs132 [unc-54p::Q35::YFP] I; artEx61 [rab-3p::hpk-1::CFP + pCFJ90 (myo-2p::mCherry)]*	n/a	9	4%	24	0.04167	0.0946	ns
	AVS835: *rmIs132 [unc-54p::Q35::YFP] I; artEx61 [rab-3p::hpk-1::CFP + pCFJ90 (myo-2p::mCherry)]*	n/a	11	38%	24	0.1009	0.1201	ns
	AVS835: *rmIs132 [unc-54p::Q35::YFP] I; artEx61 [rab-3p::hpk-1::CFP + pCFJ90 (myo-2p::mCherry)]*	n/a	13	54%	24	0.1039	0.6876	ns
Fig. 2H Line 5	AVS562: *rmIs132 [unc-54p::Q35::YFP] I*	n/a	3	0%	54	0	n/a	n/a
	AVS562: *rmIs132 [unc-54p::Q35::YFP] I*	n/a	5	2%	54	0.01852	n/a	n/a
	AVS562: *rmIs132 [unc-54p::Q35::YFP] I*	n/a	7	4%	54	0.02594	n/a	n/a
	AVS562: *rmIs132 [unc-54p::Q35::YFP] I*	n/a	9	69%	54	0.0638	n/a	n/a
	AVS562: *rmIs132 [unc-54p::Q35::YFP] I; artEx41 [rab-3p::hpk-1::CFP + pCFJ90 (myo-2p::mCherry)]*	n/a	3	0%	50	0	n/a	n/a
	AVS562: *rmIs132 [unc-54p::Q35::YFP] I; artEx41 [rab-3p::hpk-1::CFP + pCFJ90 (myo-2p::mCherry)]*	n/a	5	2%	50	0.02	0.9567	ns
	AVS562: *rmIs132 [unc-54p::Q35::YFP] I; artEx41 [rab-3p::hpk-1::CFP + pCFJ90 (myo-2p::mCherry)]*	n/a	7	4%	50	0.028	0.9382	ns
	AVS562: *rmIs132 [unc-54p::Q35::YFP] I; artEx41 [rab-3p::hpk-1::CFP + pCFJ90 (myo-2p::mCherry)]*	n/a	9	38%	50	0.0808	0.0034	**
Fig. 2J	AVS540: *rmIs132 [unc-54p::Q35::YFP] I; sid-1(pk3321)V; uIs69[unc-119p::sid-1; myo-2p::mCherry]V*	*empty vector*	3	0%	78	0	n/a	n/a
	AVS540: *rmIs132 [unc-54p::Q35::YFP] I; sid-1(pk3321)V; uIs69[unc-119p::sid-1; myo-2p::mCherry]V*	*empty vector*	5	0%	78	0	n/a	n/a
	AVS540: *rmIs132 [unc-54p::Q35::YFP] I; sid-1(pk3321)V; uIs69[unc-119p::sid-1; myo-2p::mCherry]V*	*empty vector*	7	5%	78	0.02514	n/a	n/a
	AVS540: *rmIs132 [unc-54p::Q35::YFP] I; sid-1(pk3321)V; uIs69[unc-119p::sid-1; myo-2p::mCherry]V*	*empty vector*	9	13%	78	0.04052	n/a	n/a
	AVS540: *rmIs132 [unc-54p::Q35::YFP] I; sid-1(pk3321)V; uIs69[unc-119p::sid-1; myo-2p::mCherry]V*	*empty vector*	11	23%	78	0.04801	n/a	n/a
	AVS540: *rmIs132 [unc-54p::Q35::YFP] I; sid-1(pk3321)V; uIs69[unc-119p::sid-1; myo-2p::mCherry]V*	*hpk-1*	3	0%	73	0	n/a	n/a
	AVS540: *rmIs132 [unc-54p::Q35::YFP] I; sid-1(pk3321)V; uIs69[unc-119p::sid-1; myo-2p::mCherry]V*	*hpk-1*	5	8%	73	0.03237	0.0096	**
	AVS540: *rmIs132 [unc-54p::Q35::YFP] I; sid-1(pk3321)V; uIs69[unc-119p::sid-1; myo-2p::mCherry]V*	*hpk-1*	7	33%	73	0.05536	<0.0001	****
	AVS540: *rmIs132 [unc-54p::Q35::YFP] I; sid-1(pk3321)V; uIs69[unc-119p::sid-1; myo-2p::mCherry]V*	*hpk-1*	9	84%	73	0.04368	<0.0001	****
	AVS540: *rmIs132 [unc-54p::Q35::YFP] I; sid-1(pk3321)V; uIs69[unc-119p::sid-1; myo-2p::mCherry]V*	*hpk-1*	11	95%	73	0.02682	<0.0001	****
Fig. 4B	AVS682: *rmIs132 [unc-54p::Q35::YFP] I*	n/a	5	0%	30	0	n/a	n/a
	AVS682: *rmIs132 [unc-54p::Q35::YFP] I*	n/a	7	23%	30	0.07854	n/a	n/a
	AVS682: *rmIs132 [unc-54p::Q35::YFP] I*	n/a	9	53%	30	0.09264	n/a	n/a
	AVS682: *rmIs132 [unc-54p::Q35::YFP] I*	n/a	11	93%	30	0.04632	n/a	n/a
	AVS682: *artEx62 [tph-1p::hpk-1 + pCFJ90 (myo-2p::mCherry)] line 1; rmIs132 [unc-54p::Q35::YFP] I*	n/a	5	0%	28	0	n/a	n/a

	AVS682: *artEx62 [tph-1p::hpk-1 + pCFJ90 (myo-2p::mCherry)] line 1; rmIs132 [unc-54p::Q35::YFP] I*	n/a	7	11%	28	0.05952	0.2104	ns
	AVS682: *artEx62 [tph-1p::hpk-1 + pCFJ90 (myo-2p::mCherry)] line 1; rmIs132 [unc-54p::Q35::YFP] I*	n/a	9	39%	28	0.09399	0.292	ns
	AVS682: *artEx62 [tph-1p::hpk-1 + pCFJ90 (myo-2p::mCherry)] line 1; rmIs132 [unc-54p::Q35::YFP] I*	n/a	11	75%	28	0.08333	0.0553	ns
Fig. 4D	AVS685: *rmIs132 [unc-54p::Q35::YFP] I*	n/a	5	0%	27	0	n/a	n/a
	AVS685: *rmIs132 [unc-54p::Q35::YFP] I*	n/a	7	19%	27	0.07618	n/a	n/a
	AVS685: *rmIs132 [unc-54p::Q35::YFP] I*	n/a	9	56%	27	0.09745	n/a	n/a
	AVS685: *rmIs132 [unc-54p::Q35::YFP] I*	n/a	11	93%	27	0.05136	n/a	n/a
	AVS685: *artEx65 [unc-47p::hpk-1 + pCFJ90 (myo-2p::mCherry)] line 1; rmIs132 [unc-54p::Q35::YFP] I*	n/a	5	0%	28	0	n/a	n/a
	AVS685: *artEx65 [unc-47p::hpk-1 + pCFJ90 (myo-2p::mCherry)] line 1; rmIs132 [unc-54p::Q35::YFP] I*	n/a	7	18%	28	0.1786	0.9505	ns
	AVS685: *artEx65 [unc-47p::hpk-1 + pCFJ90 (myo-2p::mCherry)] line 1; rmIs132 [unc-54p::Q35::YFP] I*	n/a	9	50%	28	0.09623	0.6867	ns
	AVS685: *artEx65 [unc-47p::hpk-1 + pCFJ90 (myo-2p::mCherry)] line 1; rmIs132 [unc-54p::Q35::YFP] I*	n/a	11	79%	28	0.07897	0.1456	ns
Fig. S5B	AVS691: *rmIs132 [unc-54p::Q35::YFP] I*	n/a	5	0%	33	0	n/a	n/a
	AVS691: *rmIs132 [unc-54p::Q35::YFP] I*	n/a	7	18%	33	0.06818	n/a	n/a
	AVS691: *rmIs132 [unc-54p::Q35::YFP] I*	n/a	9	42%	33	0.08737	n/a	n/a
	AVS691: *rmIs132 [unc-54p::Q35::YFP] I*	n/a	11	88%	33	0.0577	n/a	n/a
	AVS691: *artEx71 [eat-4p::hpk-1 + pCFJ90 (myo-2p::mCherry)] line 1; rmIs132 [unc-54p::Q35::YFP] I*	n/a	5	0%	29	0	n/a	n/a
	AVS691: *artEx71 [eat-4p::hpk-1 + pCFJ90 (myo-2p::mCherry)] line 1; rmIs132 [unc-54p::Q35::YFP] I*	n/a	7	14%	29	0.06517	0.6458	ns
	AVS691: *artEx71 [eat-4p::hpk-1 + pCFJ90 (myo-2p::mCherry)] line 1; rmIs132 [unc-54p::Q35::YFP] I*	n/a	9	41%	29	0.09308	0.935	ns
	AVS691: *artEx71 [eat-4p::hpk-1 + pCFJ90 (myo-2p::mCherry)] line 1; rmIs132 [unc-54p::Q35::YFP] I*	n/a	11	83%	29	0.07139	0.5754	ns
Fig. S5D	AVS693: *rmIs132 [unc-54p::Q35::YFP] I*	n/a	5	0%	34	0	n/a	n/a
	AVS693: *rmIs132 [unc-54p::Q35::YFP] I*	n/a	7	15%	34	0.06165	n/a	n/a
	AVS693: *rmIs132 [unc-54p::Q35::YFP] I*	n/a	9	44%	34	0.08643	n/a	n/a
	AVS693: *rmIs132 [unc-54p::Q35::YFP] I*	n/a	11	88%	34	0.05609	n/a	n/a
	AVS693: *artEx73 [cat-2p::hpk-1 + pCFJ90 (myo-2p::mCherry)] line 1; rmIs132 [unc-54p::Q35::YFP] I*	n/a	5	0%	35	0	n/a	n/a
	AVS693: *artEx73 [cat-2p::hpk-1 + pCFJ90 (myo-2p::mCherry)] line 1; rmIs132 [unc-54p::Q35::YFP] I*	n/a	7	11%	35	0.05456	0.6914	ns
	AVS693: *artEx73 [cat-2p::hpk-1 + pCFJ90 (myo-2p::mCherry)] line 1; rmIs132 [unc-54p::Q35::YFP] I*	n/a	9	40%	35	0.08402	0.7337	ns
	AVS693: *artEx73 [cat-2p::hpk-1 + pCFJ90 (myo-2p::mCherry)] line 1; rmIs132 [unc-54p::Q35::YFP] I*	n/a	11	83%	35	0.06463	0.5328	ns

Table S5. Thermotolerance assay data of all representative experiments in figures and other trials.

Figure/ Trials	Strain / Genotype	Exposure time at 35C	Survival %	Total animals (n number)	SEM	*P* value compared to control	Significance
Fig. 1C Trial 1	N2	10h	80%	220	0.0268	n/a	n/a
	hpk-1(pk1393) X	10h	48%	27	0.09799	<0.0001	****
	hpk-1(pk1393) X; artEx41 [rab-3p::hpk-1::CFP + pCFJ90 (myo-2p::mCherry)]	10h	82%	50	0.05488	Compared to *hpk-1(pk1393):* 0.0016	**
Fig. 1C Trial 2	N2	10h	64%	130	0.00251	n/a	n/a
	hpk-1(pk1393) X	10h	27%	66	0.01088	<0.0001	****
	hpk-1(pk1393) X; artEx41 [rab-3p::hpk-1::CFP + pCFJ90 (myo-2p::mCherry)]	10h	76%	75	0.00965	Compared to *hpk-1(pk1393):* <0.0001	****
Fig. 4I	AVS709: control	6h	84%	32	0.06521	n/a	n/a
	AVS709: control	8h	67%	39	0.07647	n/a	n/a
	AVS709: *artEx62 [tph-1p::hpk-1 + pCFJ90 (myo-2p::mCherry)] line 1*	6h	100%	33	0	0.0178	*
	AVS709: *artEx62 [tph-1p::hpk-1 + pCFJ90 (myo-2p::mCherry)] line 1*	8h	83%	41	0.05949	0.0955	ns
Fig. 4L	AVS710: control	6h	85%	54	0.0488	n/a	n/a
	AVS710: control	8h	69%	49	0.6652	n/a	n/a
	AVS710: *artEx65 [unc-47p::hpk-1 + pCFJ90 (myo-2p::mCherry)] line 1*	6h	89%	47	0.04546	0.5366	ns
	AVS710: *artEx65 [unc-47p::hpk-1 + pCFJ90 (myo-2p::mCherry)] line 1*	8h	69%	51	0.06562	0.9353	ns

Table S6. Induction of *hsp-16.2p::GFP* data after heat stress.

Figure/ Trials	Strain / Genotype	Conditions	GFP a.u.	Total animals (n number)	SEM	*P* value compared to control	Significance
Fig. 3C Trial 1	AVS399: *gpIs1 [hsp-16.2p::GFP]*	Heat shock 1hr at 35C, 2hr recovery at 20C	719.6	15	31.8	n/a	n/a
	AVS399: *gpIs1 [hsp-16.2p::GFP]; artEx33 [rab-3p::hpk-1::CFP +pCFJ90 (myo-2p::mCherry)]*	Heat shock 1hr at 35C, 2hr recovery at 20C	845.9	25	42.3	0.0422	*
Fig. 3C Trial 2	AVS399: *gpIs1 [hsp-16.2p::GFP]*	Heat shock 1hr at 30C, 2hr recovery at 20C	27.27	19	3.827	n/a	n/a
	AVS399: *gpIs1 [hsp-16.2p::GFP]; artEx33 [rab-3p::hpk-1::CFP +pCFJ90 (myo-2p::mCherry)]*	Heat shock 1hr at 30C, 2hr recovery at 20C	44.79	13	8.523	0.0456	*
Fig. S3C Trial 1	AVS399: *gpIs1 [hsp-16.2p::GFP]*	Heat shock 1hr at 35C, 2hr recovery at 20C	975.9	14	28.1	n/a	n/a
	AVS399: *gpIs1 [hsp-16.2p::GFP]; artEx33 [rab-3p::hpk-1::CFP +pCFJ90 (myo-2p::mCherry)]*	Heat shock 1hr at 35C, 2hr recovery at 20C	937.7	24	58.01	0.6324	ns
Fig. S3C Trial 2	AVS399: *gpIs1 [hsp-16.2p::GFP]*	Heat shock 1hr at 30C, 2hr recovery at 20C	15.26	19	1.772	0.0178	*
	AVS399: *gpIs1 [hsp-16.2p::GFP]; artEx33 [rab-3p::hpk-1::CFP +pCFJ90 (myo-2p::mCherry)]*	Heat shock 1hr at 30C, 2hr recovery at 20C	13.46	14	1.719	0.4837	ns

Table S7. Induction of autophagosomes at basal conditions data.

Figure/ Trials	Strain / Genotype	Age	# of autophagosomes	Total cells (n number)	SEM	*P* value compared to control	Significance
Fig. 3D Trial 1	AVS716: *sqIs13 [lgg-1p::GFP::lgg-1 + odr-1p::RFP]*	L4	1.576	59	0.1214	n/a	n/a
	AVS716: *artEx41 [rab-3p::hpk-1::CFP + pCFJ90 (myo-2p::mCherry)]; sqIs13 [lgg-1p::GFP::lgg-1 + odr-1p::RFP]*	L4	2.651	43	0.166	<0.0001	****
Fig. 3D Trial 2	AVS716: *sqIs13 [lgg-1p::GFP::lgg-1 + odr-1p::RFP]*	L4	1.863	80	0.1107	n/a	n/a
	AVS716: *sqIs13 [lgg-1p::GFP::lgg-1 + odr-1p::RFP]*	D1	2.597	67	0.1295	n/a	n/a
	AVS716: *artEx41 [rab-3p::hpk-1::CFP + pCFJ90 (myo-2p::mCherry)]; sqIs13 [lgg-1p::GFP::lgg-1 + odr-1p::RFP]*	L4	2.418	79	0.1355	0.0018	**
	AVS716: *artEx41 [rab-3p::hpk-1::CFP + pCFJ90 (myo-2p::mCherry)]; sqIs13 [lgg-1p::GFP::lgg-1 + odr-1p::RFP]*	D1	3.574	61	0.1661	<0.0001	****
Fig. 4J	AVS809: *sqIs13 [lgg-1p::GFP::lgg-1 + odr-1p::RFP]*	D1	1.238	80	0.09285	n/a	n/a
	AVS809: *artEx62 [tph-1p::hpk-1 + pCFJ90 (myo-2p::mCherry)] line 1; sqIs13 [lgg-1p::GFP::lgg-1 + odr-1p::RFP]*	D1	1.356	104	0.08074	0.3372	ns
Fig. 4M	AVS794: *sqIs13 [lgg-1p::GFP::lgg-1 + odr-1p::RFP]*	D1	1.672	64	0.1221	n/a	n/a
	AVS794: *artEx65 [unc-47p::hpk-1 + pCFJ90 (myo-2p::mCherry)] line 1; sqIs13 [lgg-1p::GFP::lgg-1 + odr-1p::RFP]*	D1	2.329	73	0.1051	<0.0001	****
Fig. S4A	AVS715: *sqIs24 [rgef-1p::GFP::lgg-1 + unc-122p::RFP]*	L4	16	22	0.6066	n/a	n/a
	AVS715: *artEx41 [rab-3p::hpk-1::CFP + pCFJ90 (myo-2p::mCherry)]; sqIs24 [rgef-1p::GFP::lgg-1 + unc-122p::RFP]*	L4	19.38	21	1.001	0.0057	**
Fig. S4B Trial 1	AVS716: *sqIs13 [lgg-1p::GFP::lgg-1 + odr-1p::RFP]*	L4	21	11	2.347	n/a	n/a
	AVS716: *artEx41 [rab-3p::hpk-1::CFP + pCFJ90 (myo-2p::mCherry)]; sqIs13 [lgg-1p::GFP::lgg-1 + odr-1p::RFP]*	L4	19	11	2.106	0.5331	ns
Fig. S4B Trial 2	AVS716: *sqIs13 [lgg-1p::GFP::lgg-1 + odr-1p::RFP]*	L4	23.57	23	2.51	n/a	n/a
	AVS716: *artEx41 [rab-3p::hpk-1::CFP + pCFJ90 (myo-2p::mCherry)]; sqIs13 [lgg-1p::GFP::lgg-1 + odr-1p::RFP]*	L4	21.35	17	3.313	0.5905	ns

Table S8. VD and DD motor neurons degeneration assay data.

Figure/ Trials	Strain / Genotype	Age	% of animals with axonal breaks	Total cells (n number)	SEM	*P* value compared to control	Significance
Fig. 1E	AVS602: *juIs76 [unc-25p::GFP + lin-15(+)] II*	L4	0%	17	0	**n/a**	**n/a**
	AVS602: *juIs76 [unc-25p::GFP + lin-15(+)] II*	D2	0%	20	0	**n/a**	**n/a**
	AVS602: *juIs76 [unc-25p::GFP + lin-15(+)] II*	D9	13%	23	0.0718	**n/a**	**n/a**
	AVS608: *hpk-1(pk1393); juIs76 [unc-25p::GFP + lin-15(+)] II*	L4	9%	21	0.06564	**n/a**	**n/a**
	AVS608: *hpk-1(pk1393); juIs76 [unc-25p::GFP + lin-15(+)] II*	D2	0%	23	0	**n/a**	**n/a**
	AVS608: *hpk-1(pk1393); juIs76 [unc-25p::GFP + lin-15(+)] II*	D9	72%	22	0.09719	<0.0001	****
Fig. 1F	AVS752: *artEx41 [rab-3p::hpk-1::CFP + pCFJ90 (myo-2p::mCherry)]; hpk-1(pk1393); juIs76 [unc-25p::GFP + lin-15(+)] II*	D9	0%	9	0	Compared to *AVS608:* 0.006	**
Fig. S2A	AVS602: *juIs76 [unc-25p::GFP + lin-15(+)] II*	L4	6%	17	0.05882	n/a	n/a

	AVS602: *juIs76 [unc-25p::GFP + lin-15(+)] II*	D2	5%	20	0.05	n/a	n/a
	AVS602: *juIs76 [unc-25p::GFP + lin-15(+)] II*	D9	13%	23	0.0718	n/a	n/a
	AVS608: *hpk-1(pk1393); juIs76 [unc-25p::GFP + lin-15(+)] II*	L4	10%	21	0.06564	0.6888	ns
	AVS608: *hpk-1(pk1393); juIs76 [unc-25p::GFP + lin-15(+)] II*	D2	13%	23	0.0718	0.3771	ns
	AVS608: *hpk-1(pk1393); juIs76 [unc-25p::GFP + lin-15(+)] II*	D9	45%	22	0.1087	0.0159	*

Table S9. Aldicarb assay data.

Figure/ Trials	Strain / Genotype	Hours on 1mM aldicarb	% of immobilized animals	Total cells (n number)	SEM	*P* value compared to control	Significance
Fig. 1G	N2: *wild type*	0	0%	67	0	n/a	n/a
	N2: *wild type*	1	0%	67	0	n/a	n/a
	N2: *wild type*	2	37%	67	0.05953	n/a	n/a
	N2: *wild type*	3	66%	67	0.05844	n/a	n/a
	N2: *wild type*	4	94%	67	0.02916	n/a	n/a
	N2: *wild type*	5	94%	67	0.02916	n/a	n/a
	AVS392: *hpk-1(pk1393)*	0	0%	71	0	n/a	n/a
	AVS392: *hpk-1(pk1393)*	1	0%	71	0	0.0016	**
	AVS392: *hpk-1(pk1393)*	2	14%	71	0.04158	<0.0001	****
	AVS392: *hpk-1(pk1393)*	3	31%	71	0.05527	<0.0001	****
	AVS392: *hpk-1(pk1393)*	4	54%	71	0.05961	0.0096	**
	AVS392: *hpk-1(pk1393)*	5	79	71	0.04879	0.0016	**

Table S10. Exogenous 5-HT immobilization assay data.

Figure/ Trials	Strain / Genotype	Minutes on 20mM 5-HT	% of immobilized animals	Total cells (n number)	SEM	*P* value compared to control	Significance
Fig. S2B	N2: *wild type*	0	0%	20	0	n/a	n/a
	N2: *wild type*	2	25%	20	0.09934	n/a	n/a
	N2: *wild type*	4	65%	20	0.1094	n/a	n/a
	N2: *wild type*	6	90%	20	0.06882	n/a	n/a
	N2: *wild type*	8	95%	20	0.05	n/a	n/a
	N2: *wild type*	10	95%	20	0.05	n/a	n/a

	AVS392: *hpk-1(pk1393)*	0	0%	38	0	n/a	n/a
	AVS392: *hpk-1(pk1393)*	2	63%	38	0.0793	0.0051	**
	AVS392: *hpk-1(pk1393)*	4	79%	38	0.06702	0.2566	ns
	AVS392: *hpk-1(pk1393)*	6	92%	38	0.04433	0.7905	ns
	AVS392: *hpk-1(pk1393)*	8	97%	38	0.02632	0.6455	ns
	AVS392: *hpk-1(pk1393)*	10	97	38	0.02632	0.6455	ns

References:

1. J. S. Gilleard, J. D. Barry, I. L. Johnstone, cis regulatory requirements for hypodermal cell-specific expression of the Caenorhabditis elegans cuticle collagen gene dpy-7. *Mol Cell Biol* **17**, 2301-2311 (1997).
2. P. G. Okkema, S. W. Harrison, V. Plunger, A. Aryana, A. Fire, Sequence requirements for myosin gene expression and regulation in Caenorhabditis elegans. *Genetics* **135**, 385-404 (1993).
3. M. L. Nonet *et al.*, Caenorhabditis elegans rab-3 mutant synapses exhibit impaired function and are partially depleted of vesicles. *J Neurosci* **17**, 8061-8073 (1997).
4. R. Lints, S. W. Emmons, Patterning of dopaminergic neurotransmitter identity among Caenorhabditis elegans ray sensory neurons by a TGFbeta family signaling pathway and a Hox gene. *Development* **126**, 5819-5831 (1999).
5. R. Y. Lee, E. R. Sawin, M. Chalfie, H. R. Horvitz, L. Avery, EAT-4, a homolog of a mammalian sodium-dependent inorganic phosphate cotransporter, is necessary for glutamatergic neurotransmission in caenorhabditis elegans. *J Neurosci* **19**, 159-167 (1999).
6. J. Y. Sze, M. Victor, C. Loer, Y. Shi, G. Ruvkun, Food and metabolic signalling defects in a Caenorhabditis elegans serotonin-synthesis mutant. *Nature* **403**, 560-564 (2000).
7. M. Gendrel, E. G. Atlas, O. Hobert, A cellular and regulatory map of the GABAergic nervous system of C. elegans. *Elife* **5**, (2016).
8. L. Timmons, D. L. Court, A. Fire, Ingestion of bacterially expressed dsRNAs can produce specific and potent genetic interference in Caenorhabditis elegans. *Gene* **263**, 103-112. (2001).
9. W. M. Winston, C. Molodowitch, C. P. Hunter, Systemic RNAi in C. elegans requires the putative transmembrane protein SID-1. *Science* **295**, 2456-2459 (2002).
10. R. S. Kamath *et al.*, Systematic functional analysis of the Caenorhabditis elegans genome using RNAi. *Nature* **421**, 231-237. (2003).
11. A. Calixto, D. Chelur, I. Topalidou, X. Chen, M. Chalfie, Enhanced neuronal RNAi in C. elegans using SID-1. *Nature methods* **7**, 554-559 (2010).
12. S. S. Lee, S. Kennedy, A. C. Tolonen, G. Ruvkun, DAF-16 target genes that control C. elegans life-span and metabolism. *Science* **300**, 644-647. (2003).
13. R. Das *et al.*, The homeodomain-interacting protein kinase HPK-1 preserves protein homeostasis and longevity through master regulatory control of the HSF-1 chaperone network and TORC1-restricted autophagy in Caenorhabditis elegans. *PLoS Genet* **13**, e1007038 (2017).
14. D. W. Johnson *et al.*, The Caenorhabditis elegans Myc-Mondo/Mad complexes integrate diverse longevity signals. *PLoS Genet* **10**, e1004278 (2014).
15. C. Kumsta, J. T. Chang, J. Schmalz, M. Hansen, Hormetic heat stress and HSF-1 induce autophagy to improve survival and proteostasis in C. elegans. *Nature communications* **8**, 14337 (2017).
16. H. R. Brignull, F. E. Moore, S. J. Tang, R. I. Morimoto, Polyglutamine proteins at the pathogenic threshold display neuron-specific aggregation in a pan-neuronal Caenorhabditis elegans model. *J Neurosci* **26**, 7597-7606 (2006).
17. M. I. Lazaro-Pena, A. B. Cornwell, A. V. Samuelson, Quantifying Tissue-Specific Proteostatic Decline in Caenorhabditis elegans. *Journal of visualized experiments : JoVE*, (2021).

18. J. F. Morley, H. R. Brignull, J. J. Weyers, R. I. Morimoto, The threshold for polyglutamine-expansion protein aggregation and cellular toxicity is dynamic and influenced by aging in Caenorhabditis elegans. *Proc Natl Acad Sci U S A* **99**, 10417-10422. (2002).
19. T. R. Mahoney, S. Luo, M. L. Nonet, Analysis of synaptic transmission in Caenorhabditis elegans using an aldicarb-sensitivity assay. *Nature protocols* **1**, 1772-1777 (2006).
20. K. H. Oh, H. Kim, Aldicarb-induced Paralysis Assay to Determine Defects in Synaptic Transmission in Caenorhabditis elegans. *Bio Protoc* **7**, (2017).
21. A. C. Hart, in *The C. elegans Research Community, WormBook*. (2006).